

國立交通大學

電信工程研究所

碩士論文

在第四代行動通訊中使用投機分散式空時編碼  
暨合作式自動重傳機制之跨層吞吐率分析

Cross-Layer Throughput Analysis for  
Cooperative ARQ Protocols Using  
Opportunistic DSTC in 4G Networks

研究生：陳人維

指導教授：伍紹勳

中華民國 100 年 6 月

在第四代行動通訊中使用投機分散式空時編碼暨合作式自動重傳機制  
之跨層吞吐率分析

Cross-Layer Throughput Analysis for Cooperative ARQ Protocols Using  
Opportunistic DSTC in 4G Network

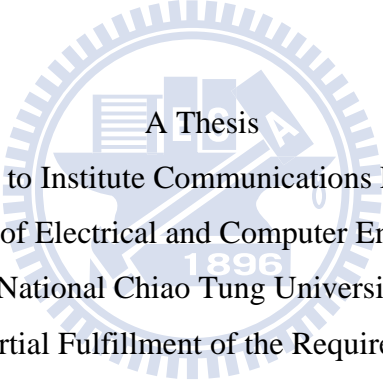
研究生：陳人維

Student : Ren-Wei Chen

指導教授：伍紹勳

Advisor : Sau-Hsuan Wu

國立交通大學  
電信工程研究所  
碩士論文



A Thesis  
Submitted to Institute Communications Engineering  
College of Electrical and Computer Engineering  
National Chiao Tung University  
in partial Fulfillment of the Requirements  
for the Degree of  
Master  
in  
Communications Engineering

June 2011

Hsinchu, Taiwan, Republic of China

中華民國一十年六月

# 在第四代行動通訊中使用投機分散式空時編碼暨合作式自動重傳機制之跨層吞吐率分析

學生：陳人維

指導教授：伍紹勳 博士

國立交通大學電信工程研究所碩士班

## 摘 要

在此篇論文中，主要是從跨層設計—實體層(PHY)和媒介擷取控制層(MAC)的角度去分析使用投機分散式空時編碼暨合作式自動重傳機制時的系統效能。為了能夠確實模擬分析媒介擷取控制層上的封包傳遞行為，針對投機分散式空時編碼暨合作式自動重傳機制，本篇論文在媒介擷取控制層提出了相容於4G網路(WiMAX)的通訊協定。此外，當使用投機分散式空時編碼(ODSTC; opportunistic distributed space-time code)技術進行傳輸時，時變衰退通道(time-varying fading channel)對於系統效能的影響在本篇論文中也會納入考慮，因此，若傳輸時節點間的交涉協商延遲(negotiating delay)大於通道的同調時間(coherence time)時，投機多樣性 (opportunistic diversity)的好處便無法完全地得到。從模擬結果可以發現，投機增益(opportunistic gain)只有當資料傳輸是在緩慢衰減通道中進行時才會存在。此外，從模擬結果也可以發現，當資料是在緩慢衰減通道中傳輸時，使用投機式阿拉蒙特時空編碼 (opportunistic Alamouti's Space-Time Code)來傳輸就能達到不錯的傳輸效能。相對於緩慢衰減通道，當資料是在快速衰減通道中傳輸時，使用投機中繼傳輸(opportunistic relaying)並不是一個有效率的方法，因此，在此情況下，隨機選擇(random selection)中繼站(RS; relay station)來進行傳輸是較為建議的方法。

# **Cross-Layer Throughput Analysis for Cooperative ARQ Protocols Using Opportunistic DSTC in 4G Network**

Student : Ren-Wei Chen

Advisor : Dr. Sau-Hsuan Wu

Institute of Communications Engineering  
National Chiao Tung University

## **ABSTRACT**

The thesis investigates the performance of cooperative Automatic-Repeat-reQuest protocol (ARQ) with the opportunistic distributed space-time coding scheme from the perspective of the cross-layer (Media Access Control, MAC, layer and Physical, PHY, layer) design. Based on the concept of opportunistic relaying for ARQ, the corresponding MAC protocols which are compatible to the WiMAX relay-assisted network are proposed in this work. In addition, the time-varying fading channel is considered when using the ODSTC scheme. Thus, the full opportunistic diversity possibly is not available when the negotiating delay is greater than the channel coherence interval. The simulation results show that the opportunistic gain only exists in slow fading channel, and using distributed Alamouti code is good enough through exploiting the opportunistic gain. On the other hand, the opportunistic relaying is not an efficiency scheme in fast fading channel. Therefore, random selection for choosing RS is recommended when the fading effect is serious.

## 誌 謝

能夠順利地完成這篇碩士論文，我必須要感謝很多人指導與幫助。首先，我由衷地感謝我的指導教授—伍紹勳老師，感謝老師在我的碩士求學過程中，有系統地把我訓練成一位研究人員，這其中的訓練，除了專業知識的指導與傳授以外，老師在研究上的嚴謹積極態度，更是我效法的對象，讓我明白面對問題以及處理問題的正確態度。在研究之餘，老師也非常照顧學生的生活起居，除了不定時關心學生生活外，也會盡可能地把可運用的資源都投注在學生身上，讓學生能夠無後顧之憂地專注於自己的研究。在此，我要深深地感謝老師為學生所做的一切。除了伍紹勳老師以外，我也非常感謝趙禧綠老師，感謝老師在學生的研究過程中給予精闢的建議與指導。

再來，我必須要感謝邱新粟學長、曾俊凱學長以及邱麟凱學長，給予我在研究以及生活上的幫助。由其是邱新粟學長，在我的碩士求學階段中，不厭其煩的教導我，並且適時地給予我中肯的建議。除了上述的學長外，實驗室的戰友們在精神上的支持與鼓勵，更是我能夠一步一步往前走的動力來源，很慶幸自己曾經是 MBWCL 的一員。

我還要感謝周遭一直關心我的朋友，不間斷地給予我支持與鼓勵。另外我也要感謝交大管樂團提供我吹奏樂器的機會，讓我在心情煩悶時，能夠透過音樂演奏來抒發情緒。

最後我要感謝我的父母，在我從小到大的求學路程中，一直不計代價地栽培我包容我，是我在求學路上最溫暖的避風港，讓我能夠有勇氣面對各種挑戰，非常感謝我的父母對我所做的一切。

誌於 2011.06 新竹 交通大學

人維

# Contents

<b>1</b>	<b>Introduction</b>	<b>1</b>
<b>2</b>	<b>Preliminary</b>	<b>5</b>
2.1	Frame Structure for WiMAX System . . . . .	5
2.2	Band AMC Permutation Scheme . . . . .	6
2.3	Transparent RS Mode, RS Grouping and DSTC . . . . .	7
<b>3</b>	<b>System Model and Setting for Cross-Layer Analysis</b>	<b>8</b>
3.1	System Model . . . . .	8
3.1.1	Channel Uncertainty . . . . .	10
3.1.2	Markov Fading Channel Model . . . . .	11
<b>4</b>	<b>Opportunistic Relaying Protocols for ARQ</b>	<b>13</b>
4.1	The Behavior of BS and SS in Opportunistic Relaying . . . . .	13
4.2	Type-A ARQ Protocol . . . . .	15
4.3	Type-B ARQ Protocol . . . . .	16
4.4	Type-C ARQ Protocol . . . . .	18
<b>5</b>	<b>Packet Error Analysis</b>	<b>25</b>

5.1	Outage Probability for Opportunistic Relaying Scheme . . . . .	25
5.2	Definition of Error Packet in NS2 Simulation . . . . .	27
<b>6</b>	<b>Cross-layer Throughput Analysis</b>	<b>30</b>
6.1	Throughput Analysis . . . . .	30
6.1.1	Throughput Analysis for the Type-A ARQ Protocol . . . . .	31
6.1.2	Throughput Analysis for the Type-B ARQ Protocol . . . . .	33
6.2	Queue Stability Analysis . . . . .	34
6.3	Rate Assignment . . . . .	36
6.3.1	Proposed Rate Adaptation Scheme . . . . .	36
<b>7</b>	<b>Simulation Results</b>	<b>39</b>
7.1	Performance Evaluation of Multiple Relays Assisted Network . . . . .	40
7.1.1	The Evaluation of Rate Adaptation Scheme for the Case Without RS . . . . .	41
7.1.2	Relay-Assisted Network . . . . .	43
<b>8</b>	<b>Conclusions</b>	<b>52</b>
<b>9</b>	<b>Appendices</b>	<b>54</b>
9.1	Appendix 1 . . . . .	54
9.1.1	The Outage Probability of BS-RSs link and BS-SS link . . . . .	54
9.1.2	The Outage Probability of RSs-SS link . . . . .	56

# List of Figures

2.1	Frame structure of WiMAX network. . . . .	6
2.2	BandAMC permutation scheme. . . . .	6
3.1	The system model for M RSs and single SS case. . . . .	9
3.2	The transition diagram for Markov fading channel. . . . .	12
4.1	The time diagram for BS and SS in opportunistic relaying. . .	14
4.2	The time diagram in Type-A ARQ protocol. . . . .	15
4.3	The time diagram for RS in Type-B ARQ protocol. . . . .	17
4.4	The time diagram in Type-C ARQ protocol. . . . .	19
4.5	Flow chart for BS. . . . .	20
4.6	Flow chart for SS . . . . .	21
4.7	Flow chart for Type-A ARQ. . . . .	22
4.8	Flow chart for Type-B ARQ. . . . .	23
4.9	Flow chart for Type-C ARQ. . . . .	24
5.1	The outage state in Markov fading channel. . . . .	28
7.1	The simulation parameters . . . . .	40



7.2	Network topology for without RS case. The coverage of BS is 3 km. . . . .	41
7.3	Compare the rate adaption schemes in different fading speed. .	42
7.4	Topology for the case with multiple RSs. The coverage is 3 km and 8km for suburban and rural area, respectively . . . . .	43
7.5	The throughput enhancement by single RS. . . . .	44
7.6	The throughput performance with different number of RSs, fading speed. . . . .	45
7.7	The throughput performance for different types of protocol in different fading speed. . . . .	46
7.8	The throughput with different types of protocol in different $i$ when $V=120$ km/hr. . . . .	47
7.9	The throughput with different types of protocol in different $i$ when $V=3$ km/hr. . . . .	48
7.10	The recommended opportunistic relaying scheme. . . . .	49
7.11	The difference between ideal numerical result and simulation results. . . . .	50
7.12	The comparisons between ideal numerical result and practical simulation result . . . . .	51

## Abstract

The thesis investigates the performance of cooperative Automatic-Repeat-reQuest protocol (ARQ) with the opportunistic distributed space-time coding scheme from the perspective of the cross-layer (Media Access Control, MAC, layer and Physical, PHY, layer) design. Based on the concept of opportunistic relaying for ARQ, the corresponding MAC protocols which are compatible to the WiMAX relay-assisted network are proposed in this work. In addition, the time-varying fading channel is considered when using the ODSTC scheme. Thus, the full opportunistic diversity possibly is not available when the negotiating delay is greater than the channel coherence interval. The simulation results show that the opportunistic gain only exists in slow fading channel, and using distributed Alamouti code is good enough through exploiting the opportunistic gain. On the other hand, the opportunistic relaying is not an efficiency scheme in fast fading channel. Therefore, random selection for choosing RS is recommended when the fading effect is serious.

# Chapter 1

## Introduction

The bandwidth requirements of user is growing over time. In order to meet the needs of users, cooperative communication is widely discussed and investigated to improve the wireless transmission quality. In the cooperative communication, the data transmission is completed by the collaboration of source and multiple helpers (*i.e.*, relay stations). Through the help from relay station (RS), the spatial diversity gain is achievable no matter how many antennas are equipped at source node and destination node. In addition to spatial diversity, cooperative communication also can enhance throughput by reducing the path-loss effect on transmission, [1] and [2]. In general, the appropriate RS is located between the source and destination node. Under the situation, the path loss effect on source-relay (S-R) links and relay-destination (R-D) links is smaller than the direct link. Thus, the higher data rate can be used for transmission in the two links of S-R ( $R_{SR}$ ) and R-D ( $R_{RD}$ ) than S-D link ( $R_{SD}$ ) possibly. If  $\frac{1}{R_{SR}} + \frac{1}{R_{RD}} < \frac{1}{R_{SD}}$ , the two-way transmission will provide the enhancement in system throughput. Comparing the cost,

convenience for deployment and the enhancement of system performance, the cooperative relaying is an efficiency scheme to enhance the performance and it is already development the relaying strategies is proposed in the 4G standards, [3] and [4].

As introduced earlier, cooperative communication is able to obtain the spatial diversity via the help from RS. In order to exploit the full spatial diversity, distributed space-time code (DSTC) is used in the cooperative communication system, [5]. However, to exploit the full spatial diversity, the size of DSTC has to be adjusted adaptively with the number of available RS before each transmission. Thus, the negotiation for adaptive adjusting is a complex task when multiple relays are involved in the transmission. In order to reduce the complexity, the opportunistic relaying(OR) scheme which only choose the best RS to send data is proposed in [6]. The chosen RS owns the best channel quality to SS. Through mechanism of RS selection, the full spatial diversity still can be achieved even if the transmission is completed by single RS. The idea of OR can be extended to the case of distributed Alamouti code in RS transmissions, [7]. Through combining the ideas of OR scheme and Automatic-Repeat-reQuest(ARQ) scheme, the opportunistic ARQ relaying protocol where the RS is used for retransmission is proposed in [8], and three types of opportunistic ARQ relaying protocols are designed with different complexity of RS. From the view point of system effectiveness, [8] shows that the most effective ARQ relaying scheme is not always the most complex scheme or using all the available RSs.

The aforementioned methods are only discussed from the viewpoint of physical (PHY) layer. Thus, the negotiating delay and overhead is not con-

sidered while feeding back the channel state information (CSI). However, the wireless channel is time-varying in the real environment. The responding CSI is not reliable when the feedback delay is much longer than the coherence time of channel variation. Due to the obsolete responding CSI, the source node cannot select RSs accurately while using the OR scheme. Consequently, the delay effect on feedback is necessary to be considered while designing the cooperative communication system with OR scheme. In order to evaluate the delay effect, the cross-layer protocol design for RS selection in cooperative communication system is vital.

Medium access control (MAC) protocol design for cooperative communication is more and more popular in recent years, [1] [2] [9]. In ad hoc network, [1] and [2] exploit the two-way transmission by RS forwarding to enhance the system capacity. However, the RS selection is performed before transmission. Thus, the RS selection may not adapt to dynamical channel condition and network topology. In order that the RS selection can adapt to dynamic environment, based on [1] the MAC protocol for opportunistic relaying is proposed in [9]. The MAC protocol with RS is proposed in the 4G standards, IEEE 802.16m [3] and 3GPP LTE-Advanced [4], for the centralized network. Based on the standard IEEE 802.16j [10], [11] offers a MAC protocol which can enable multiple RSs to forward data by DSTC scheme.

In contrast to the ad hoc network, the investigations of opportunistic relaying in the centralized network are less. In addition, the effect of the time-varying fading channel is not considered when evaluating the performance of the OR system. In this work, we follow the ideas of opportunistic relaying in [8] to develop corresponding MAC protocols for ARQ based on the WiMAX

standard [10]. In addition, the effect of the time-varying fading channel is considered in our numerical analysis and simulations. In other words, the timeliness of feedback CSI will be influenced by the time-varying channel characteristics, and the opportunistic diversity might loss as well and even degenerate to the case of that DSTC scheme. From the perspective of the transmission efficiency, opportunistic relaying is not an efficient scheme to enhance throughput in fast fading channel.



# Chapter 2

## Preliminary

In this work, the opportunistic relaying ARQ protocols are developed according to IEEE 802.16j [10]. In other words, the scheme of handshakes and negotiations among BS, RSs and SSs should follow the WiMAX specifications in order that the opportunistic relaying ARQ protocols are compatible to the WiMAX system. Thus, a briefly review of important features for WiMAX system is needed and will be introduced in this chapter.

### 2.1 Frame Structure for WiMAX System

The frame structure of a traditional WiMAX relay-assisted network is basically composed by downlink (DL) access zone, DL relay zone, uplink (UL) access zone and UL relay zone. The map broadcasting is included in DL access zone where and sent by BS. In this work to a time division duplexing

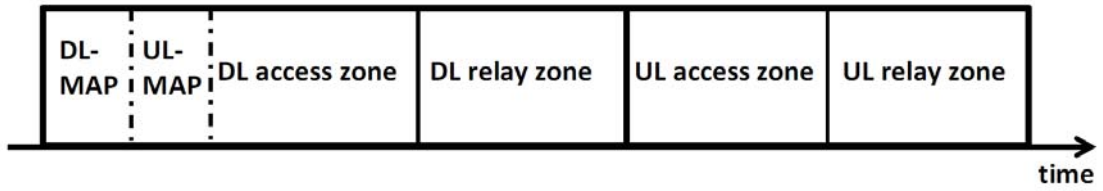


Figure 2.1: Frame structure of WiMAX network.

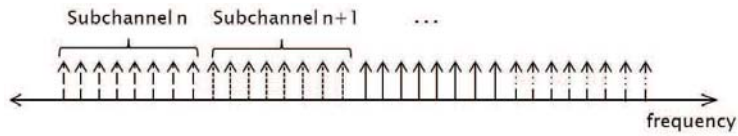


Figure 2.2: BandAMC permutation scheme.

WiMAX system, the map broadcasting, DL and UL data transmissions are implemented in different time durations, and the frame structure can be illustrated in Fig 2.1. The BS is able to indicate RSs and SS when and which subcarrier to operate by the map in relay-assisted network. Generally, the DL access zone is used for BS to send packets and the UL access zone is used for SS to contact with BS. The RSs are able to forward packet to SS and BS in DL relay zone and UL relay zone, respectively.

## 2.2 Band AMC Permutation Scheme

The transmission of WiMAX relay-assisted network is based on the orthogonal frequency-division multiple access (OFDMA) system. Therefore, BS allocates the transmitting resource for each user on frequency domain and time domain. There are some permutation schemes which are used to group subcarriers to subchannel. Band adaptive modulation and coding (Band



AMC) is one of the permutation scheme which makes the adjacent subcarriers form a subchannel, as illustrated in Fig. 2.2. Because the subchannel is composed by the adjacent subcarriers, the channel gain of each subcarrier in the same subchannel is similar. The characteristic of the same channel gain is conducive to enhance throughput by resource allocation. Thus, the Band AMC is used in this work.

## 2.3 Transparent RS Mode, RS Grouping and DSTC

According to the purposes of network design, WiMAX provides two kinds of RS modes, namely non-transparent relay and transparent relay mode. The users which are located out of the cell coverage are able to contact with BS by the relaying of Non-transparent RS. Thus, Non-transparent relay mode is used to extend the cell coverage. On the other hand, the users which are served by transparent RS are able to communicate with BS directly. Thus, the transparent relay mode is dedicated for throughput enhancement instead of coverage extension. Moreover, BS is able to request multiple RSs to form a RS group. Through the RS group, the DSTC scheme can be applied to the RS transmissions. In this work, throughput enhancement via RSs' help is the primary goal. Therefore, all RSs belong to the transparent relay mode in this investigation.

# Chapter 3

## System Model and Setting for Cross-Layer Analysis

Following the WiMAX standards, the system model will be introduced in the beginning of this chapter. The lower bound of channel capacity with considering channel uncertainty effect and Markov fading channel model will be offered in the end of the chapter.

### 3.1 System Model

We consider a WiMAX relay-assisted network, as illustrated in Fig. 3.1, which is composed by one BS,  $M$  RSs and one SS. Each node in the network only equips with single antenna for transmission, and the  $M$  RSs belong to the same RS group. In this work, all investigations only focus on the DL data transmission with using decoded-and-forward (DF) relaying scheme in one subchannel. For simplicity, we assume that the broadcasting map can

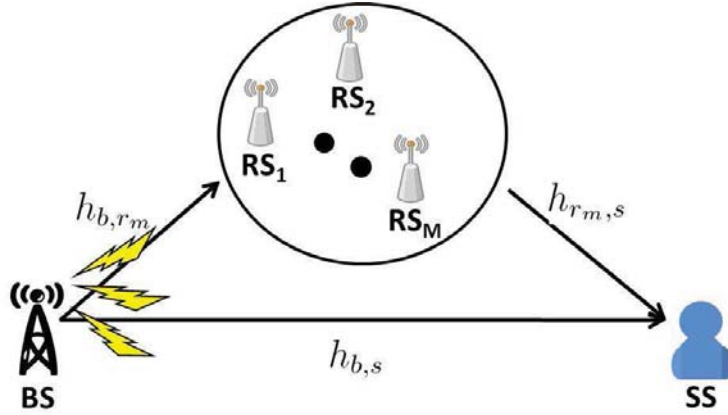


Figure 3.1: The system model for  $M$  RSs and single SS case.

always be correctly received at RSs and SS, and the BS can also receive the acknowledgements and feedback information from RSs and SS without error. In addition, we further assume that the  $M$  RSs are geometrically close to each other, and thus, the  $M$  RSs receive the same average signal power, denoted by  $P_{b,r}$ , from BS. Similarly, the received signal power at SS from each RS,  $P_{r,s}$ , is considered the same.

Let  $h_{b,s}$  be the channel coefficient between the BS and SS, and let  $h_{b,r_m}$  be the channel coefficient between the BS and  $RS_m$ ,  $\forall m \in \{1, \dots, M\}$ . As for the data transmission, the received signals at SS and  $RS_m$  from BS, denoted by  $y_{b,s}$  and  $y_{b,r_m}$ , respectively, can be modeled as

$$y_{b,s} = \sqrt{P_{b,s}}h_{b,s}x + n_s \quad (3.1)$$

$$y_{b,r_m} = \sqrt{P_{b,r}}h_{b,r_m}x + n_r \quad (3.2)$$

where  $P_{b,s}$  stands for the average received signal power at SS from BS, and the

noise at the SS and RS, denoted by  $n_s$  and  $n_r$ , are modeled as  $\sim \mathcal{CN}(0, N_0)$ .

Before transmitting data, the BS is able to ask the RS group to monitor the data transmission. The RSs which decode the packet correctly from BS will form a RS set, namely decoding set, denoted as  $\mathcal{S}_{\mathcal{D}}$ . The RSs in  $\mathcal{S}_{\mathcal{D}}$  are able to resend data when the SS fails in decoding from BS. In order to enhance the performance on retransmissions, the BS is able to select at most  $i$  RSs among  $\mathcal{S}_{\mathcal{D}}$  to retransmit by Opportunistic DSTC (ODSTC) scheme, denoted ODSTC $i$ . If the cardinality of the decoding set, denoted as  $\mathcal{D}$ , is less than  $i$ , then all the RSs in the decoding set have to forward together with using DSTC. When  $\mathcal{S}_{\mathcal{D}} = \emptyset$ , which represents that all RSs decode the packet unsuccessfully, the BS still needs to rebroadcast the packet by itself until that  $\mathcal{S}_{\mathcal{D}} \neq \emptyset$  or the SS succeeds in decoding. To the SS, the received signals from RS $_m$ ,  $y_{r_m,s}$ , is modeled as

$$y_{r_m,s} = \sqrt{P_{r,s}} h_{r_m,s} x + n_s \quad (3.3)$$

where  $h_{r_m,s}$  denotes the channel coefficient between the SS and RS $_m$ .

Based on the this cooperative system, to characterize the fading speed effect from the perspective of channel capacity, [12] shows the lower bound of capacity with considering the channel uncertainty. In addition, the results of [13] are referred to simulate the practical fading channel in this work.

### 3.1.1 Channel Uncertainty

In the real environment of wireless communication, the receiver cannot always obtain the exact channel information. The receiver has to use the previ-

ous channel information to estimate the present channel condition. Thus, the estimation error of channel will exist at the receiver when receiving signal. In [12], the authors provide the lower bound of capacity with considering the channel uncertainty. Assume that the received packet occupies  $T_p$  OFDM symbols, the channel capacity is modified as

$$C(T_p, \rho) \geq \frac{1}{T_p} \sum_{n=1}^{T_p} \log_2 \left\{ 1 + \frac{a^{2(n-1)} \rho |H|^2}{1 + [1 - a^{2(n-1)}] \rho} \right\} \quad (3.4)$$

where  $C(T_p, \rho)$  denotes the average capacity during the  $T_p$  OFDM symbols.  $|H|^2$  denotes the channel gain at the first OFDM symbol.  $a^2 \triangleq \frac{R_{hh}(1)}{R_{hh}(0)}$  denotes the estimation error variance,  $R_{hh}(\tau) \triangleq J_o\{2\pi f_m T_s \tau\}$  and  $f_m \triangleq \frac{f_c \cdot v}{c}$ .  $f_c$ ,  $v$  and  $c$  denotes the center frequency, receiver moving speed and the speed of light, respectively.

### 3.1.2 Markov Fading Channel Model

In the typical wireless mobile channel, the characters of time varying channel will seriously influence the performance of transmission. In order to simulate the time-varying channel, the fading channel in this work is modeled as finite state Markov chain, [13]. Thus, the channel is transferred from continuous to discrete. Through quantization, the channel is divided into  $K$  Markov states, such as  $\omega_1, \omega_2, \omega_3, \dots, \omega_K$ , and these  $K$  states form the  $\Omega$ ,  $\Omega \triangleq \{\omega_1, \omega_2, \omega_3, \dots, \omega_K\}$ . Let  $P_T\{\omega_n | \omega_{n+1}\}$  denotes the transition probability from state  $\omega_{n+1}$  to state  $\omega_n$ . The transition diagram of Markov fading channel is illustrated in Fig. 3.2. In this work, the derivations of the parameters such as  $\omega_i$  and  $P_T\{\omega_n | \omega_{n+1}\}$  are based on the results of [13].

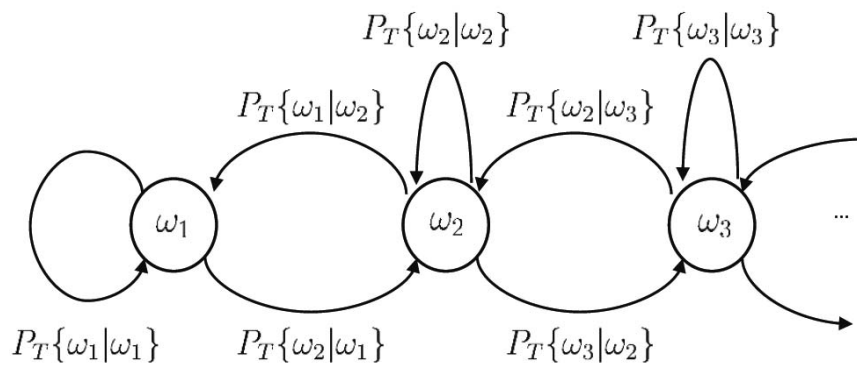


Figure 3.2: The transition diagram for Markov fading channel.

# Chapter 4

## Opportunistic Relaying

### Protocols for ARQ

As introduced earlier, there are three opportunistic ARQ relaying schemes proposed in [8] with different complexity for RS. Based on the idea, the corresponding ARQ relaying MAC protocols are introduced in this chapter.

#### 4.1 The Behavior of BS and SS in Opportunistic Relaying

For these three opportunistic relaying schemes, the behavior of SS and BS are the same. The corresponding time diagram is illustrated in Fig. 4.1 and the frame structure is the simplified version of Fig. 2.1. In the beginning of the first frame, the BS will broadcast the MAP which records the transmitting rules of this MAC frame. After MAP broadcasting, the BS

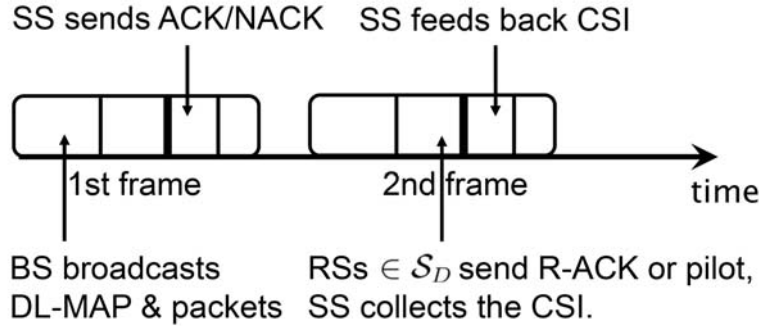


Figure 4.1: The time diagram for BS and SS in opportunistic relaying.

will send the packets to the SS and the RSs will monitor the transmission. If the SS decodes the packet correctly, the SS will feedback ACK. Otherwise, the SS will feedback NAK. In addition to the BS, the RSs are able to receive the ACK/NAK packet. If the RS which belongs to  $\mathcal{S}_D$  receives the NAK from SS, the RS will send R-ACK to the SS in the next DL relay zone. By receiving the R-ACK, the SS can obtain the list of available RSs and the CSI of the RS-SS link. Then, SS will feedback the CSI and the list of available RSs in the UL access zone. According to the these feedbacks, the BS can select RS for retransmission accurately.

In the time diagram, the description is from the perspective of the transmitted packet. The detailed process of opportunistic relaying protocol for BS and SS is illustrated in the individual flow chart, Fig. 4.5 and Fig. 4.6, respectively. In the flow chart, the corresponding time for the step is marked in the left timeline. The BS has to broadcast the MAP in the head of each MAC frame. Then, the BS will send packets and receive ACK in the DL access zone and UL access zone, respectively. For SS, the critical step for



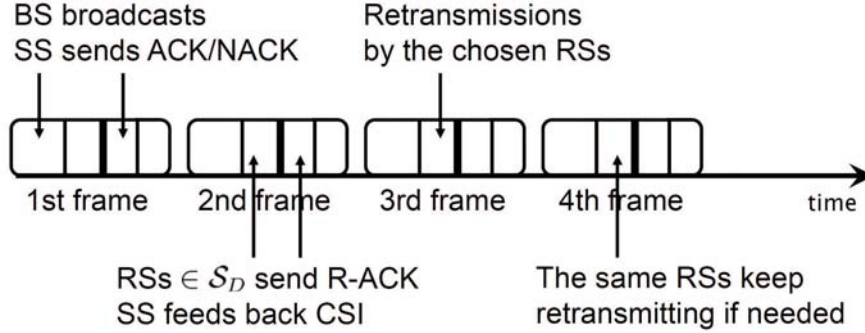


Figure 4.2: The time diagram in Type-A ARQ protocol.

opportunistic relaying is feeding back the CSI and the list of available RSs to the BS. Thus, the SS will feed back the information of RSs which is collected in the DL relay zone to the BS in the UL access zone. Other processes in the flow chart have been introduced in the description for time diagram.

## 4.2 Type-A ARQ Protocol

As introduced earlier, the RSs need to send R-ACK or pilot in order that BS is able to get the CSI and the list of  $\mathcal{S}_D$  for each retransmitting packet. The RS can use the R-ACK to notify the BS that this RS belongs to the  $\mathcal{S}_D$ . Therefore, the available RSs only need to send R-ACK in the first negotiation. If RS has notified BS by the R-ACK, the RS is able to help SS collect the CSI by sending the smaller packet (i.e. pilot packet). Under the mechanism of collecting CSI, the time diagram of RS for Type-A ARQ protocol is illustrated in the Fig. 4.2.

In the first frame, if the BS sends the packet to the SS unsuccessfully, the SS will send NAK in the UL access zone. After receiving the NAK, the

available RSs will send R-ACK in the next DL relay zone. Through the feedbacks from SS in the second frame, the BS is able to select the best  $i$  RSs among the  $\mathcal{S}_{\mathcal{D}}$  to resend the packet in the third frame. The results of RS selection will be recorded in the DL-MAP and broadcasted by BS in the head of the third frame. Then, the chosen RSs will follow the indications of the DL-MAP to resend the packet in the DL relay zone. In the Type-A ARQ protocol, the retransmissions of the packet only rely on these  $i$  RSs, and the same  $i$  RSs need to retransmit the packet again in the subsequent frames if the packet is sent unsuccessfully in the third frame.

The flow chart of RS is illustrated in Fig. 4.7. The RS will receive the MAP from BS in each frame. Because the BS only selects the RSs in the first retransmission, the un-chosen RSs drop the packet while obtaining the indications of RS selection from DL-MAP. In the indicated time, the RSs will overhear the designated transmission and reserve it if the decoding is correct at the RS. In the DL relay zone, the chosen RSs will resend the packet according to the indications of DL-MAP. Then, the RSs will check the size of buffer. The nonempty buffer represents that these packets need to retransmit by the RSs. Therefore, the RSs will help SS to collect the CSI and the list of available RSs by sending R-ACK or pilot. In the UL access zone, the RS possibly receives ACK or NAK from the SS. If the ACK packet is received, the corresponding packet in the buffer will be dropped by RS.

### 4.3 Type-B ARQ Protocol

The primary difference between Type-A ARQ protocol and Type-B ARQ

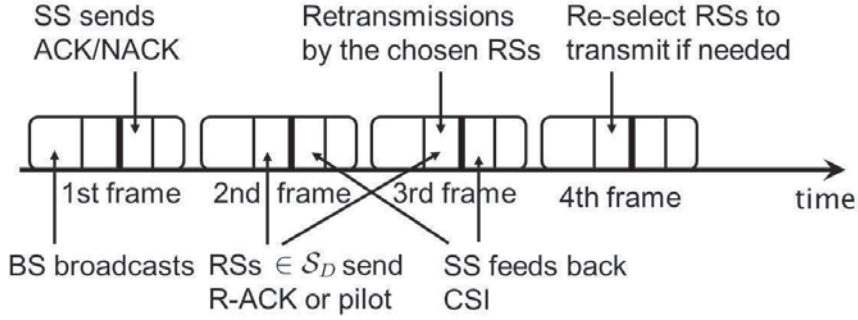


Figure 4.3: The time diagram for RS in Type-B ARQ protocol.

protocol is in RS reselection, the BS will reselect the RSs in each time of retransmission in Type-B ARQ protocol. Based on the idea of Type-B ARQ Protocol in [8], the time diagram of RS is illustrated in the Fig. 4.3. Similar to Fig. 4.2, the RSs  $\in \mathcal{S}_D$  send the R-ACK to SS in the second frame if the SS decodes the packet unsuccessfully in the first frame. Then, BS requests the best  $i$  RSs to resend packet in the third frame. In addition, the RS will send the pilot packet in the third frame because the buffer is not empty now. The SS needs to feed back CSI to the BS in the UL access zone. The BS can renew the CSI of RS-SS links via receiving the feedbacks. If the SS still can not decode the packet correctly from RS, the BS is able to reselect the appropriate  $i$  RSs according to the latest CSI. These  $i$  RSs which are chosen in the third frame will resend the packet again in the fourth frame.

The difference between Type-B and Type-A protocol is only in the RS reselection. Thus, the unchosen RSs still need to reserve the packet in the Type-B protocol. The flow chart for RS is illustrated in Fig. 4.8. The RS does not drop packet when receiving the DL-MAP in the DL access zone. Except for the packet dropping at the unchosen RSs, other behavior of RS

in Type-B protocol is the same as that of Type-A protocol.

## 4.4 Type-C ARQ Protocol

In the Type-C ARQ protocol, the mechanism of RS reselection is reserved. Moreover, the RSs are able to overhear each other in the DL relay zone. The time diagram is illustrated in Fig. 4.4 which is almost the same as that of Type-B in Fig. 4.3, except for the third frame. In the third frame, the chosen  $i$  RSs will resend the packet in the DL relay zone. At the same time, the RSs  $\notin \mathcal{S}_{\mathcal{D}}$  are able to overhear the transmission. Through the overhearing, the size of  $\mathcal{S}_{\mathcal{D}}$  possibly grows after each time of retransmission until all  $M$  RSs  $\in \mathcal{S}_{\mathcal{D}}$ .

The flow chart of RS is illustrated in Fig. 4.9. The flow chart of Type-C ARQ protocol is similar to the Type-B ARQ protocol except for the behavior in the DL relay zone. If the RS is not asked to transmit packet, it is allowed to overhear the packet from other RSs which are retransmitting packet. If the RS  $\notin \mathcal{S}_{\mathcal{D}}$  decodes the packet correctly, the RS is able to help the retransmissions in the following retransmission.

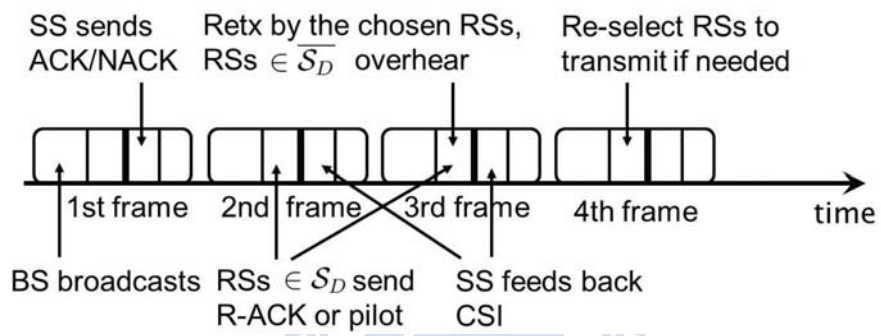
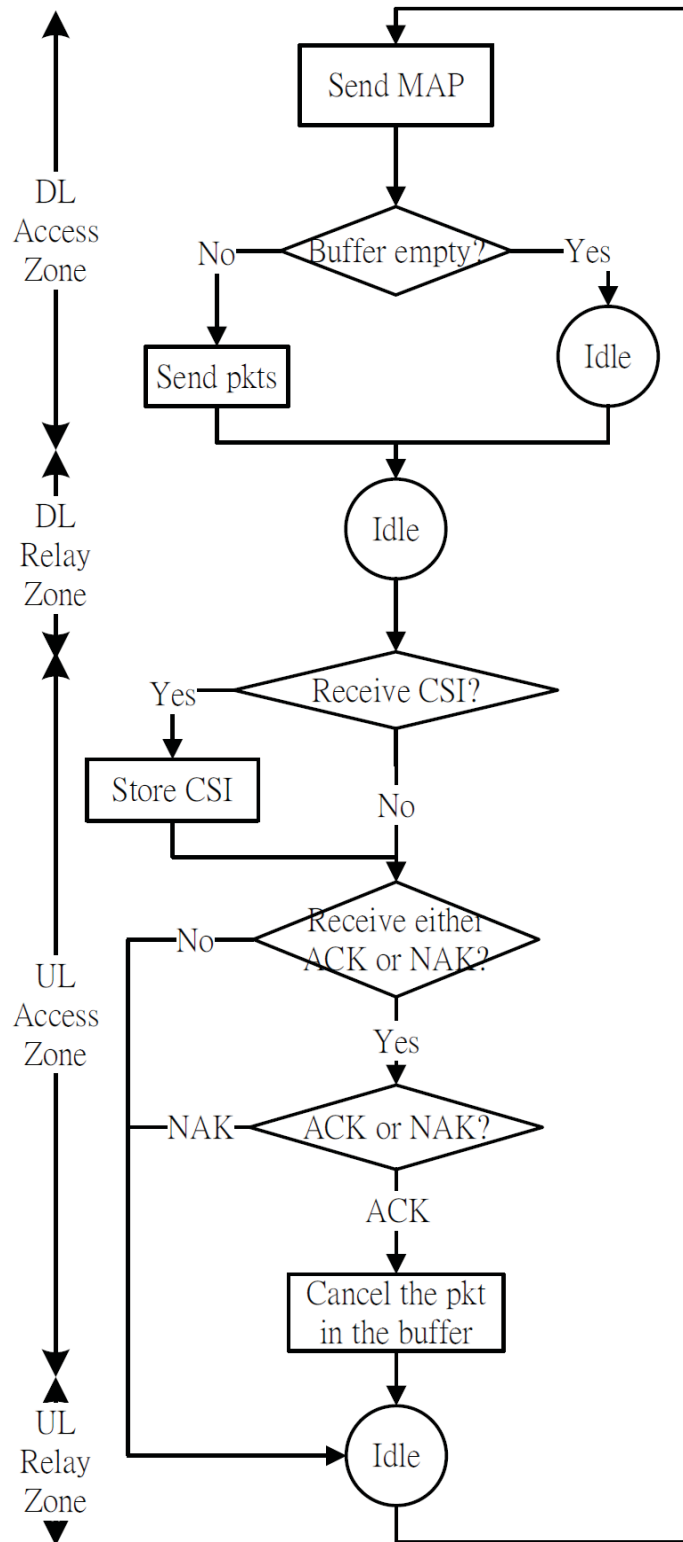


Figure 4.4: The time diagram in Type-C ARQ protocol.



20  
Figure 4.5: Flow chart for BS.

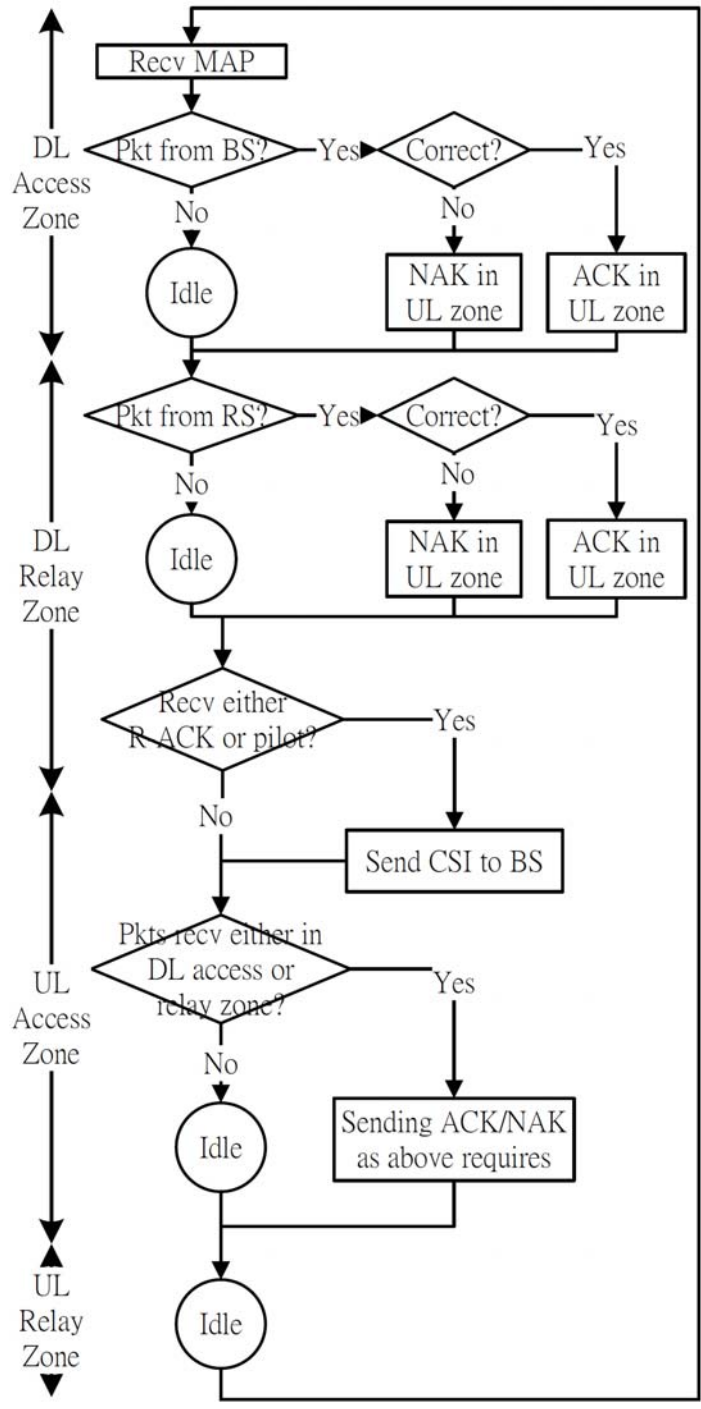


Figure 4.6: Flow chart for SS .

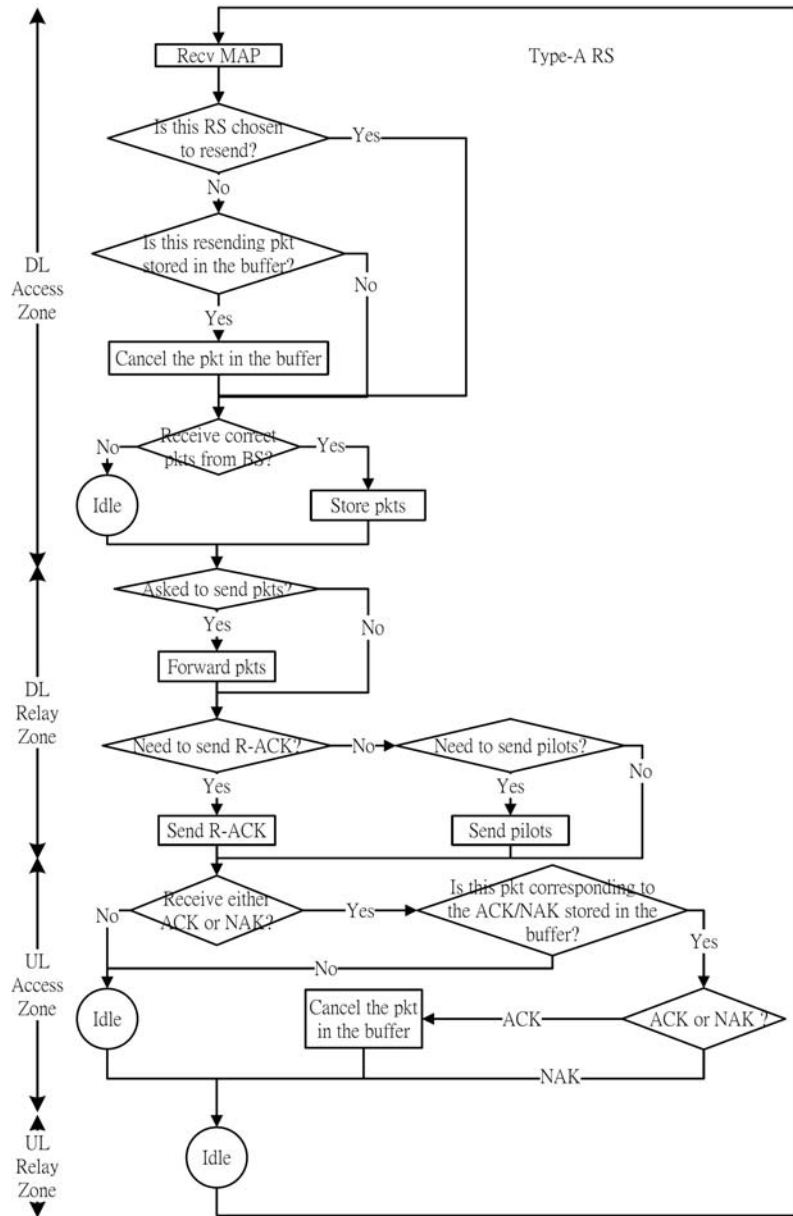


Figure 4.7: Flow chart for Type-A ARQ.



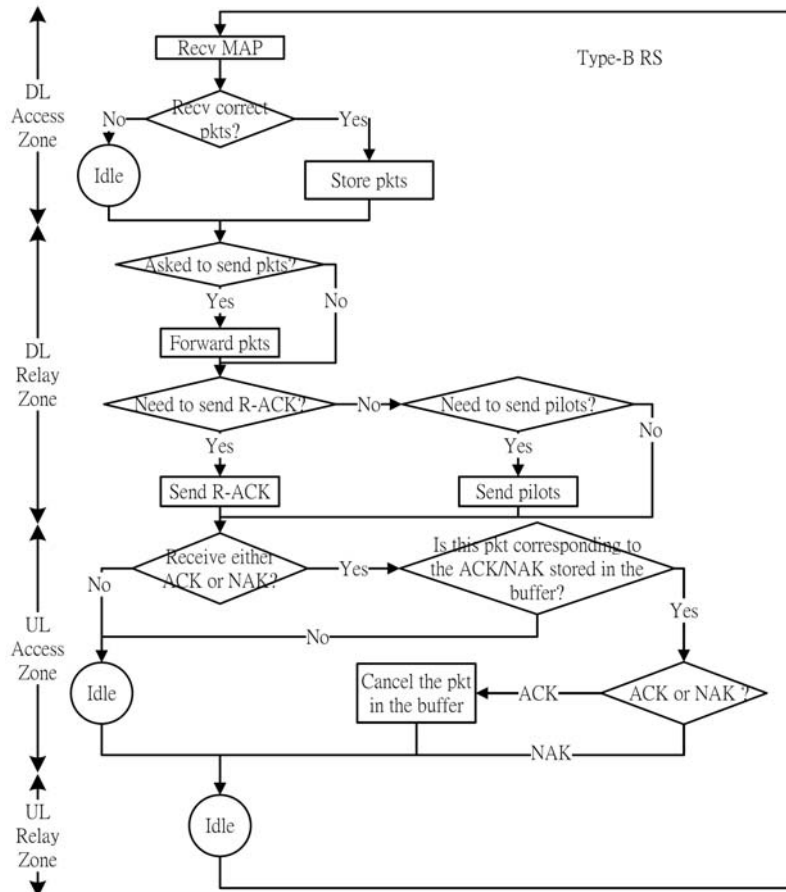


Figure 4.8: Flow chart for Type-B ARQ.

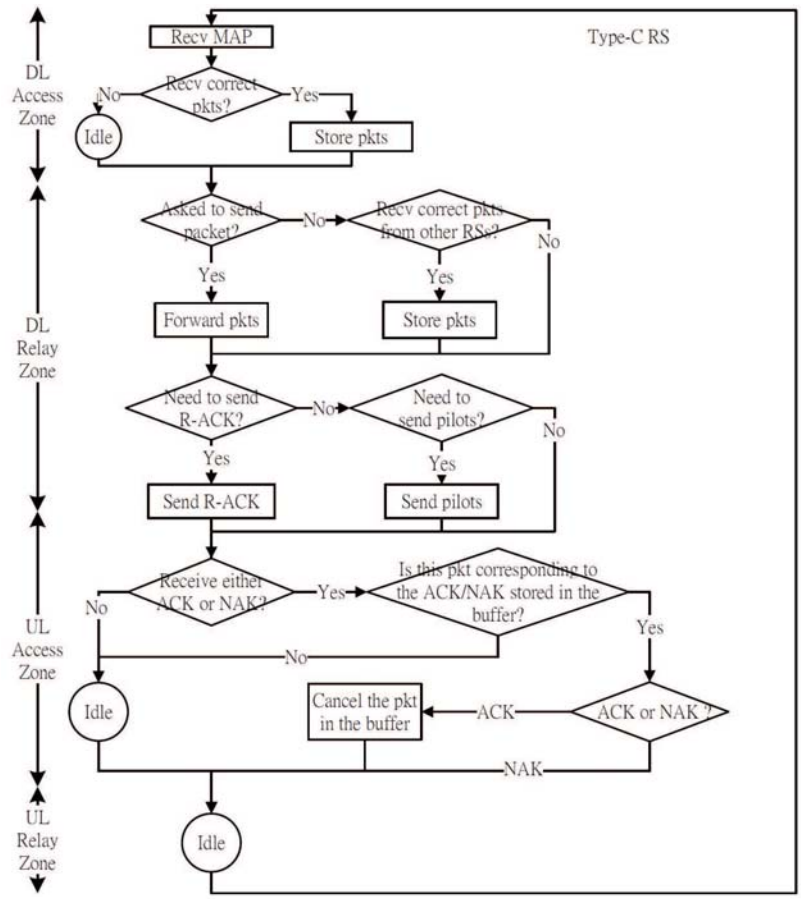


Figure 4.9: Flow chart for Type-C ARQ.

# Chapter 5

## Packet Error Analysis

In order to simplify the complexity of investigations, the analysis and simulations are based on the view point of outage probability. In this chapter, we will analyze the outage probability of opportunistic relaying scheme and introduce the definition of error packet in the simulation.

### 5.1 Outage Probability for Opportunistic Relaying Scheme

The outage probability of the received packet whose packet duration is  $T_p$  OFDM symbols is defined as

$$P \triangleq \Pr \{R > C(T_p, \rho)\} \quad (5.1)$$

where  $P$  denotes the outage probability,  $R$  denotes the data rate of the packet and  $C(T_p, \rho)$  denotes the channel capacity whose definition is in (3.4). According to (5.1), the outage probability of the BS-SS link and RS-SS link are denoted as  $P_{b,s}$  and  $P_{b,r}$  which can be shown as

$$\begin{aligned} P_{b,s}(R_b, \rho_{b,s}) &= \Pr \{R_b > C_{b,s}(T_p, \rho_{b,s})\} \\ &= \Pr \left\{ R_b > \frac{1}{T_p} \sum_{n=1}^{T_p} \log \left\{ 1 + \frac{a^{2(n-1)} |h_{b,s}|^2 \rho_{b,s}}{1 + (1 - a^{2(n-1)}) \rho_{b,s}} \right\} \right\} \end{aligned} \quad (5.2)$$

$$\begin{aligned} P_{b,r}(R_b, \rho_{b,r}) &= \Pr \{R_b > C_{b,r}(T_p, \rho_{b,r})\} \\ &= \Pr \left\{ R_b > \frac{1}{T_p} \sum_{n=1}^{T_p} \log \left\{ 1 + \frac{a^{2(n-1)} |h_{b,r}|^2 \rho_{b,r}}{1 + (1 - a^{2(n-1)}) \rho_{b,r}} \right\} \right\} \end{aligned} \quad (5.3)$$

where  $R_b$  denotes the data rate for BS transmission.

In the opportunistic relaying protocol for ARQ, the BS is able to select multiple RSs to resend the packet by ODSTC scheme according to the channel quality of RS-SS link. Let  $\mathcal{H} \triangleq \{|H_1|^2, |H_2|^2, \dots, |H_d|^2, d = \mathcal{D}\}$  denotes the set of the channel gain from the RSs in  $\mathcal{S}_{\mathcal{D}}$ .  $\mathcal{D}$  denotes the cardinality of  $\mathcal{S}_{\mathcal{D}}$ . Then, sorting the elements of  $\mathcal{H}$  in ascending order into  $\mathcal{X} \triangleq \{|X_1|^2, |X_2|^2, \dots, |X_d|^2, \}$  such that  $|X_k|^2 \geq |X_j|^2$ , if  $k > j$ . Under the situation, the outage probability by using ODSTC scheme is given by

$$\begin{aligned} &P_{\mathcal{O}_i|\mathcal{D}}(R_r, \rho_{r,s}|d) \\ &\triangleq \Pr \left\{ \mathcal{O}_i \triangleq \frac{1}{T_p} \sum_{n=1}^{T_p} \log \left( 1 + \frac{a^{2(n-1)} \sum_{j=d_i}^d |X_j|^2 \rho_{r,s}}{1 + (1 - a^{2(n-1)}) \rho_{r,s}} \right) < R_r \mid d \geq 1 \right\} \end{aligned} \quad (5.4)$$

where  $d_i \triangleq \max\{1, d-i+1\}$  and  $R_r$  denotes the data rate for RS transmission.

From the Theorem 1 in [8], the complementary cumulative density function

(CCDF) of  $\sum_{j=d_i}^d |X_j|^2$  is given by

$$\begin{aligned}
& \Pr \left\{ \sum_{j=d_i}^d |X_j|^2 > z \right\} \\
&= \sum_{j=1}^{d-i} a_j e^{\left(\frac{-c_j}{i} z\right)} \times \frac{1}{(i-1)!} \int_0^z e^{(b_j t) t^{(i-1)}} dt + \sum_{k=0}^{i-1} e^{(-z)} \frac{(z)^k}{k!} \\
&= \sum_{j=1}^{d-i} a_j e^{\left(\frac{-c_j}{i} z\right)} \times \frac{1}{(-b_j)^i} \left[ 1 - e^{b_j z} \sum_{\ell=0}^{i-1} \frac{(-b_j z)^\ell}{\ell!} \right] + \sum_{k=0}^{i-1} e^{(-z)} \frac{(z)^k}{k!} \quad (5.5)
\end{aligned}$$

where  $a_j \triangleq \frac{1}{d-j+1} \frac{d!}{i!} \frac{(-1)^{d-i-j}}{(j-1)!(d-i-j)!}$ ,  $b_j \triangleq \frac{d-i-j+1}{i}$  and  $c_j \triangleq d-j+1$ .

Therefore, the cumulative density function (CDF) is given by

$$\begin{aligned}
& \Pr \left\{ \sum_{j=d_i}^d |X_j|^2 < z \right\} \\
&= 1 - P \left\{ \sum_{j=d_i}^d |X_j|^2 > z \right\} \\
&= 1 - \sum_{j=1}^{d-i} a_j e^{\left(\frac{-c_j}{i} z\right)} \times \frac{1}{(-b_j)^i} \left[ 1 - e^{b_j z} \sum_{\ell=0}^{i-1} \frac{(-b_j z)^\ell}{\ell!} \right] - \sum_{k=0}^{i-1} e^{(-z)} \frac{(z)^k}{k!} \quad (5.6)
\end{aligned}$$

## 5.2 Definition of Error Packet in NS2 Simulation

In Section 3.1.2, the finite state Markov model is used to simulate the fading channel, and channel is divide to K states. Based on the perspective

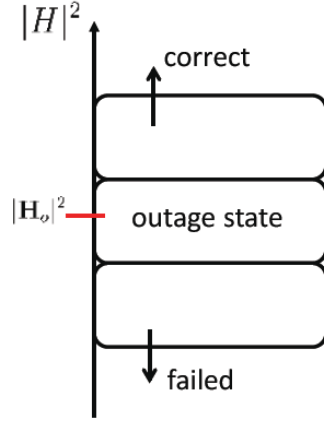


Figure 5.1: The outage state in Markov fading channel.

of outage probability, the received packet will be considered outage if the channel state of the received packet is below to the outage channel state which included the outage threshold,  $|H_o|^2$ , in Fig. 5.1. Otherwise, the packet is successful when the channel state is greater than outage channel state. However, it is difficult to define whether the packet is correct or not if the channel state of the received packet is same with the outage state. Therefore, we need to develop a scheme to solve the problem.

Let  $\{\Gamma_0, \Gamma_1, \dots, \Gamma_K\}$  denote the threshold of Markov channel state. If the channel gain of received packet is said to be in channel state  $\omega_i, i = 1, 2, 3 \dots K$ , the channel gain is located in the range  $[\Gamma_{i-1}, \Gamma_i)$ .

Assuming that SS receives a packet whose data rate is  $R$  and packet duration is  $T_p$  from the best  $i$  RSs by ODSTC scheme. Let the channel gain from the  $j$ -th RS is  $|H_j|^2$ , and  $|H_j|^2$  is in the channel state  $\omega_{D_j}, \omega_{D_j} \in \Omega$ . Based on these receiving channel state,  $\omega_{D_1}, \omega_{D_2}, \dots, \omega_{D_i}$ , the outage

probability of the received packet is given by

$$\begin{aligned}
& P_{out} (R_r, \rho_{r,s} | \omega_{D_1}, \dots, \omega_{D_i}) \\
&= \Pr \{ C_{r,s} (T_p, \rho_{r,s}, i) < R_r | \omega_{D_1}, \dots, \omega_{D_i} \} \\
&= \frac{1}{\pi_{D_1} \pi_{D_2} \dots \pi_{D_i}} \\
&\cdot \Pr \left\{ \frac{1}{T_p} \sum_{n=1}^{T_p} \log \left\{ 1 + \frac{a^{2(n-1)} \sum_{j=1}^i |H_j|^2 \rho_{r,s}}{1 + (1 - a^{2(n-1)}) \rho_{r,s}} \right\} < R_r, \omega_{D_1}, \dots, \omega_{D_i} \right\}
\end{aligned} \tag{5.7}$$

where the  $\pi_{D_i} \triangleq e^{-\Gamma_{D_i}} - e^{-\Gamma_{D_i-1}}$  denotes the steady-state probability of state  $\omega_{D_i}$ . Let  $|H_S|^2 = \sum_{j=1}^i |H_j|^2$  and  $\sigma_n = \frac{a^{2(n-1)} \rho_{r,s}}{1 + (1 - a^{2(n-1)}) \rho_{r,s}}$ . Assume  $R_r = \frac{1}{T_p} \sum_{n=1}^{T_p} \log \{1 + \sigma_n |H_o|^2\}$ ,

$$\begin{aligned}
& \Pr \left\{ \frac{1}{T_p} \sum_{n=1}^{T_p} \log \left\{ 1 + \frac{a^{2(n-1)} \sum_{j=1}^i |H_j|^2 \rho_{r,s}}{1 + (1 - a^{2(n-1)}) \rho_{r,s}} \right\} < R_r, \omega_{D_1}, \dots, \omega_{D_i} \right\} \\
&= \Pr \left\{ \frac{1}{T_p} \sum_{n=1}^{T_p} \log \{1 + \sigma_n |H_S|^2\} < \frac{1}{T_p} \sum_{n=1}^{T_p} \log \{1 + \sigma_n |H_o|^2\}, \omega_{D_1}, \dots, \omega_{D_i} \right\} \\
&= \Pr \{ |H_S|^2 < |H_o|^2, \omega_{D_1}, \dots, \omega_{D_i} \} \\
&= \Pr \{ |H_1|^2 + |H_2|^2 + \dots + |H_i|^2 < |H_o|^2, \omega_{D_1}, \dots, \omega_{D_i} \} \\
&= \int_{\omega_{D_1}} \int_{\omega_{D_2}} \dots \int_{\omega_{D_i}} e^{-x_1} e^{-x_2} \dots e^{-x_i} dx_1 dx_2 \dots dx_i
\end{aligned} \tag{5.8}$$

# Chapter 6

## Cross-layer Throughput Analysis

From the above chapter, we have known the mechanism of opportunistic relaying MAC ARQ protocols in Chapter 4 and the outage probability of opportunistic relaying in Chapter 5 with considering the queue stability of RS. Based on the throughput and queue stability analysis, the rate adaptation scheme is developed in the end of the chapter.

### 6.1 Throughput Analysis

Throughput is a significant criterion for network designer to evaluate the system performance. In our investigations, we define the throughput,  $\Psi$ , as

$$\Psi \triangleq \frac{N_{pkt}}{E[\tau]} \quad (\text{bits/sec/Hz}) \quad (6.1)$$



where  $N_{pkt}$  denotes packet length in bits and  $E[\tau]$  denotes average transmission time for successfully sending a packet to SS, and it is given by

$$E[\tau] = \sum_{n_b=0}^{\infty} \sum_{n_r=0}^{\infty} ((1 + n_b)T_p + n_r T_r) \mathcal{P}_S \{n_b, n_r\} \quad (6.2)$$

where  $n_b$  and  $n_r$  denotes the transmission times for BS and RS.  $\mathcal{P}_S \{n_b, n_r\}$  denotes the probability of decoding packets successfully at SS after  $n_b$  and  $n_r$  times of retransmissions by BS and RS, respectively.

### 6.1.1 Throughput Analysis for the Type-A ARQ Protocol

In Type-A ARQ protocol, the unchosen RS will drop the packet. Therefore, these unchosen RSs lose the abilities to resend the packet in the following retransmissions. In other words, the O-DSTC scheme is just implemented at the first retransmission. the  $\mathcal{P}_S \{n_b, n_r\}$  in Type-A scheme is denoted as  $\mathcal{P}_{A,S} \{n_b, n_r\}$  and the throughput of Type-A is given by

$$\Psi_A = \frac{N_{pkt}}{E[\tau_A]} = \frac{N_{pkt}}{\sum_{n_b=0}^{\infty} \sum_{n_r=0}^{\infty} ((1 + n_b)T_p + n_r T_r) \mathcal{P}_{A,S} \{n_b, n_r\}} \quad (6.3)$$

By [14],  $\Psi_A$  can be given by solving  $E[\tau_A]$  which is shown as

$$\begin{aligned}
E[\tau_A] &= \cdot \{T_b[1 - P_{b,s}(R_b, \rho_{b,s})P_{\mathcal{D}}(0)] \\
&\quad \cdot \{1 + \mathcal{A} + n_{s,c}\mathcal{A}^* + n_{s,c}n_{r,c}P_{b,s}^{n_{r,c}}(R_b, \rho_{b,s})P_{\mathcal{D}}^{n_{s,c}}(0)\mathcal{A}_2\} \\
&\quad + T_r P_{b,s}(R_b, \rho_{b,s}) \{1 + \mathcal{A}\} \sum_{d=1}^M P_{\mathcal{D}} \left[ 1 + n_{s,c} \frac{P_{\mathcal{O}_i|D}(R_r, \rho_{r,s}|d)}{1 - P_{STC}(R_r, \rho_{r,s}|d)} \right]
\end{aligned} \tag{6.4}$$

where

$$\mathcal{A} = \frac{P_{\mathcal{D}}(0)f(n_{s,c}, n_{r,c})}{1 - P_{b,s}^{n_{r,c}}(R_b, \rho_{b,s})P_{\mathcal{D}}^{n_{s,c}}(0)} \tag{6.5}$$

$$\mathcal{A}^* = \frac{P_{\mathcal{D}}(0)f^*(n_{s,c}, n_{r,c})}{1 - P_{b,s}^{n_{r,c}}(R_b, \rho_{b,s})P_{\mathcal{D}}^{n_{s,c}}(0)} \tag{6.6}$$

$$\mathcal{A}_2 = \frac{P_{\mathcal{D}}(0)f(n_{s,c}, n_{r,c})}{[1 - P_{b,s}^{n_{r,c}}(R_b, \rho_{b,s})P_{\mathcal{D}}^{n_{s,c}}(0)]^2} \tag{6.7}$$

$$f(n_{s,c}, n_{r,c}) = \sum_{j=1}^{n_{r,c}} P_{b,s}^j(R_b, \rho_{b,s}) \cdot P_{\mathcal{D}}(0)^{(j-1)\lfloor \frac{n_{s,c}}{n_{r,c}} \rfloor} \tag{6.8}$$

$$f^*(n_{s,c}, n_{r,c}) = \sum_{j=1}^{n_{r,c}} j \cdot P_{b,s}^j(R_b, \rho_{b,s}) \cdot P_{\mathcal{D}}(0)^{(j-1)\lfloor \frac{n_{s,c}}{n_{r,c}} \rfloor} \tag{6.9}$$

$$P_{\mathcal{D}}(d) = C_d^M (1 - P_{b,r}(R_b, \rho_{b,r}))^d P_{b,r}(R_b, \rho_{b,r})^{M-d} \tag{6.10}$$

$$P_{STC}(R_r, \rho_{r,s}|d) = P_{\mathcal{O}_i|D}(R_r, \rho_{r,s}|i) \tag{6.11}$$

$n_{s,c}$  and  $n_{r,c}$  denotes the coherence interval of channel for SS and RS, respectively.

### 6.1.2 Throughput Analysis for the Type-B ARQ Protocol

In Type-B ARQ protocol, all RSs will keep reserving the packet no matter whether the RS is chosen to retransmit or not. Therefore, BS can reselect the best  $i$  RSs in each retransmission. Under the situation,  $\mathcal{P}_{\mathcal{B},\mathcal{S}}\{n_b, n_r\}$  is given by

$$\Psi_B = \frac{N_{pkt}}{E[\tau_B]} = \frac{N_{pkt}}{\sum_{n_b=0}^{\infty} \sum_{n_r=0}^{\infty} ((1+n_b)T_p + n_r T_r) \mathcal{P}_{\mathcal{B},\mathcal{S}}\{n_b, n_r\}} \quad (6.12)$$

By [14], the  $E[\tau_B]$  is given by

$$\begin{aligned} E[\tau_B] &= T_b [1 - P_{b,s}(R_b, \rho_{b,s}) P_{\mathcal{D}}(0)] \\ &\quad \cdot \{1 + \mathcal{A} + n_{s,c} \mathcal{A}^* + n_{s,c} n_{r,c} P_{b,s}^{n_{r,c}}(R_b, \rho_{b,s}) P_{\mathcal{D}}^{n_{s,c}}(0) \mathcal{A}_2\} \\ &\quad + T_r P_{b,s}(R_b, \rho_{b,s}) \{1 + \mathcal{A}\} \sum_{d=1}^M P_{\mathcal{D}} \left[ 1 + n_{s,c} \frac{P_{\mathcal{O}_i|D}(R_r, \rho_{r,s}|d)}{1 - P_{\mathcal{O}_i|D}(R_r, \rho_{r,s}|d)} \right] \end{aligned} \quad (6.13)$$

The throughput analysis of Type-C ARQ protocol is too complex if the number of retransmitting is unlimited. Thus, the derivation of the Type-C ARQ protocol is not the scope of this work.

## 6.2 Queue Stability Analysis

In this work, the RS is not able to reject the relaying requirements from BS. Thus, the queue of RS is possibly unstable which means the size of queue will keep growing with time if the packet arrival rate,  $\lambda_r$ , is greater than packet departure rate,  $\mu_r$ , at RS. However, the queue stability is not considered when selecting the data rate to maximize throughput in PHY layer. Thus, the chosen data rate will so optimistic that the queue of RS is possibly unstable. In order to avoid the queue of RS unstable, the queue stability analysis is considered in our cross-layer design while selecting the data rate.

Assuming that the observation point of RS queue is in the beginning of MAC frame, the packet arrival event for RS only happens when RS receives the packet correctly but SS is failed. Therefore, the packet arrival rate represents the number of packet which is received correctly by RS but unsuccessfully by SS from BS in each MAC frame. By referring the [14], the packet arrival rate of RS queue can be given by

$$\lambda_r = \frac{P_{b,s}(R_b, \rho_{b,s})[1 - P_{\mathcal{D}}(0)]}{P_{b,s}(R_b, \rho_{b,s})[1 - P_{\mathcal{D}}(0)] + n_{r,c} \{1 - P_{b,s}(R_b, \rho_{b,s})[1 - P_{\mathcal{D}}(0)]\}} \quad (6.14)$$

Similar to arrival rate, the packet departure rate of RS queue represents the number of packet which is sent successful by RS in each MAC frame. The

definitions of departure rate is given by

$$\begin{aligned}\mu_r &= \frac{1}{\text{average service time for one packet by RS}} \\ &= \frac{1}{E[S_r]} \quad (\text{pkts/MAC frame})\end{aligned}\quad (6.15)$$

According to the definitions, the derivations of average service time,  $E[S_r]$ , for different ARQ protocols are introduced in this section.

### I. Departure rate of RS in Type-A ARQ protocol

Following (6.15), the departure rate in Type-A which is denoted as  $\mu_{r,A}$  is defined by

$$\mu_{r,A} \triangleq \frac{1}{E[S_{r,A}]} \quad (6.16)$$

where  $E[S_{r,A}]$  denotes the average duration for sending a packet by RS when adopting Type-A MAC protocol. By referring to [14],  $E[S_{r,A}]$  is given by

$$E[S_{r,A}] = \frac{1}{[1 - P_D(0)]} \sum_{d=1}^M P_D(d) \left[ 1 + n_{s,c} \frac{P_{O_i|D}(R_r, \rho_{r,s}|d)}{1 - P_{STC}(R_r, \rho_{r,s}|d)} \right] \quad (6.17)$$

### II. Departure rate of RS in Type-B ARQ protocol

The derivations of Type-B departure rate,  $\mu_{r,B}$ , are similar to Type-A protocol. Defines  $\mu_{r,B} \triangleq 1/E[S_{r,B}]$  where  $E[S_{r,B}]$  denotes the average duration for successfully sending a packet to SS by RS. By referring to [14],

$E[S_{r,B}]$  is given by

$$E[S_{r,B}] = \frac{1}{[1 - P_{\mathcal{D}}(0)]} \sum_{d=1}^M P_{\mathcal{D}}(d) \left[ 1 + n_{s,c} \frac{P_{\mathcal{O}_i|D}(R_r, \rho_{r,s}|d)}{1 - P_{\mathcal{O}_i|D}(R_r, \rho_{r,s}|d)} \right] \quad (6.18)$$

## 6.3 Rate Assignment

In WiMAX specification, there are seven kinds of data rate are supported and these data rate are composed of a set which is denoted by  $\mathcal{S}_{\mathcal{R}}$ . After deriving the throughput formula, we want to develop a scheme of rate selection. By the scheme of rate selection, we can select the appropriate rates from  $\mathcal{S}_{\mathcal{R}}$  for RS and BS which can maximize the throughput under stability constraints of RS queue. Unfortunately, we cannot directly derive the appropriate rate due that we do not have the closed form of outage probability. Nevertheless, we still developed a rate adaption schemes, namely proposed rate scheme.

### 6.3.1 Proposed Rate Adaptation Scheme

Due to the complex capacity formula, we cannot derive the closed form expression of the outage probability. Therefore, we use the simplified capacity formula to substitute for the original capacity formula(3.4).

$$\begin{aligned} \tilde{C}(T_p, \rho, \beta) &= \beta \cdot \log_2 \{1 + |H|^2 \rho\} + (1 - \beta) \cdot \log_2 \left\{ 1 + \frac{a^{2(T_p-1)} |H|^2 \rho}{1 + (1 - a^{2(T_p-1)}) \rho} \right\} \\ &= \beta \cdot \log_2 \{1 + |H|^2 \rho\} + (1 - \beta) \cdot \log_2 \{1 + \sigma_{T_p} |H|^2\} \end{aligned} \quad (6.19)$$

where  $\sigma_{T_p} \triangleq \frac{a^{2(T_p-1)}\rho}{1+(1-a^{2(T_p-1)})\rho}$ . The weighting coefficient,  $\beta$ , is a real number. In order to obtain the closed form expression of (6.19), we let  $\beta = 0.5$  or  $\beta = \frac{1}{3}$ . The outage probability  $\widetilde{P}(R, \rho, \beta)$  is given by

$$\widetilde{P}(R, \rho, \beta) \triangleq Pr \left\{ \widetilde{C}(T_p, \rho, \beta) < R \right\} \quad (6.20)$$

The derivations of outage probability for BS-SS link ( $\widetilde{P}_{bs}$ ), BS-RSs link ( $\widetilde{P}_{br}$ ) and RSs-SS link ( $\widetilde{P}_{rs}(i, D)$ ) when  $\beta = 0.5$  are recorded in the Appendix I and given by

$$\widetilde{P}_{b,s}(R_b, \rho_{b,s}, 0.5) = 1 - e^{-\frac{-(\rho_{b,s} + \sigma_{T_p}) + \sqrt{(\rho_{b,s} + \sigma_{T_p})^2 + 4(2^{2R_b} - 1)\rho_{b,s}\sigma_{T_p}}}{2\rho_{b,s}\sigma_{T_p}}} \quad (6.21)$$

$$\widetilde{P}_{b,r}(R_r, \rho_{b,r}, 0.5) = 1 - e^{-\frac{-(\rho_{b,r} + \sigma_{T_p}) + \sqrt{(\rho_{b,r} + \sigma_{T_p})^2 + 4(2^{2R_b} - 1)\rho_{b,r}\sigma_{T_p}}}{2\rho_{b,r}\sigma_{T_p}}} \quad (6.22)$$

$$\begin{aligned} \widetilde{P}_{\mathcal{O}_i|D}(R_r, \rho_{r,s}, 0.5|d) &= 1 - \sum_{k=0}^{i-1} e^{(-\eta_{r,s})} \frac{(\eta_{r,s})^k}{k!} \\ &\quad - \sum_{j=1}^{d-i} a_j e^{\left(\frac{-e_j}{i}\eta_{r,s}\right)} \cdot \frac{1}{(-b_j)^i} \left[ 1 - e^{b_j\eta_{r,s}} \sum_{\ell=0}^{i-1} \frac{(-b_j\eta_{r,s})^\ell}{\ell!} \right] \end{aligned} \quad (6.23)$$

By the derivations of outage probability, the throughput,  $\widetilde{\Psi}$ , can be derived from 6.1 by replacing  $P_{b,s}(R_b, \rho_{b,s}), P_{b,r}(R_b, \rho_{b,r}), P_{\mathcal{O}_i|D}(R_r, \rho_{r,s}|d)$  with  $\widetilde{P}_{b,s}(R_b, \rho_{b,s}, \beta), \widetilde{P}_{b,r}(R_b, \rho_{b,r}, \beta)$  and  $\widetilde{P}_{\mathcal{O}_i|D}(R_r, \rho_{r,s}, \beta|d)$ . Through the formula of  $\widetilde{\Psi}$ , the appropriated data rate,  $\widetilde{R}_b^*$  and  $\widetilde{R}_r^*$ , for BS and RS is given by

$$\begin{aligned} &\max_{\widetilde{R}_b^*, \widetilde{R}_r^* \in \mathcal{S}_{\mathcal{R}}} \quad \widetilde{\Psi} \\ &s.t. \quad \widetilde{\lambda}_R < \widetilde{\mu}_r \end{aligned}$$

Similar to  $\tilde{\Psi}$ ,  $\tilde{\lambda}_R$  and  $\tilde{\mu}_r$  are derived by modifying the (6.14) and (6.15), respectively. we hope we can select the suitable data rate for BS and RS from  $\mathcal{S}_R$  which can maximize  $\tilde{\Psi}$ .





# Chapter 7

## Simulation Results

In order to examine the performance of all ARQ protocols in different fading speed, we use NS2, Network Simulation 2, to simulate the behavior of these ARQ protocols. The simulator of relay-assisted network is developed based on the structure of WiMAX module from National Institute of Standards and Technology (NIST). The parameters in the simulations are summarized in Fig.7.1. The transmitted power of BS, RS and SS is 40 W, 4 W and 0.2W, and the height of antenna for BS, RS and SS is 32m, 10m and 1.5m. The bandwidth of the OFDMA system is 10 MHz and the frame duration is 5 ms. We used the BAND-AMC permutation scheme to group sub-carriers into sub-channels. There are 18 sub-carriers in each sub-channel, but only 16 sub-carriers are used for data transmission. The remaining 2 sub-carriers are pilot carriers which can be used for channel estimation.

In order to simulate the practical path-loss effect, the path-loss model which is the function of propagation distance, central frequency, antenna height and terrain is referred from [15] and [16]. The relay-assisted network

BS transmit power:	40 Watts
RS transmit power:	4 Watts
SS transmit power:	0.2 Watts
Noise power:	-104 dBm
Carrier frequency:	2.5 GHz
BS antenna height:	32 m
RS antenna height:	10 m
SS antenna height:	1.5 m
FFT size:	1024
OFDM symbol duration:	102.8 $\mu$ s
The number of OFDM symbols per MAC frame:	47
MAC frame duration:	5 ms
Packet size:	6 OFDM symbols

Figure 7.1: The simulation parameters

is simulated in both suburban and rural environment. In suburban area, Type-B and Type-F model in [16] are used to simulate the path-loss effect. According to the height of the antenna at transmitter and receiver, Type-B path-loss model is used for BS-SS and RS-SS links and Type-F path-loss model is used for RS-SS and RS-RS. For the rural case, the path-loss model is referred from [15].

## 7.1 Performance Evaluation of Multiple Relays Assisted Network

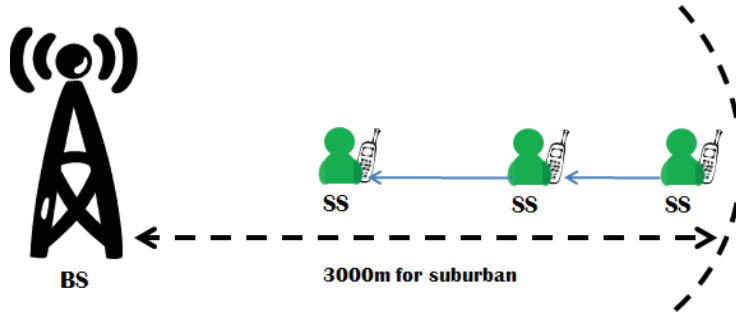


Figure 7.2: Network topology for without RS case. The coverage of BS is 3 km.

### 7.1.1 The Evaluation of Rate Adaptation Scheme for the Case Without RS

The network topology for the case without RS is illustrated in the Fig. 7.2. Based on the topology, three kinds of rate adaption scheme, intuitive rate scheme, proposed rate scheme and adaptive rate rate, are used for transmission and the simulation results are illustrated in Fig. 7.3. In the simulation, there are two kinds of moving speed,  $V=3$  km/hr and  $V=120$  km/hr, for user while received packets, and the X-axis denotes the averaged received SNR at SS. The higher moving speed represents the fading effect is more serious. Thus, the throughput in the  $V=120$  km/hr case is lower than the  $V=3$  km/hr case for any kind of rate adaption scheme.

The purpose of rate adaption scheme is maximizing the throughput. In order to evaluate the performance of these rate adaption schemes, the results by exhaustive search are used as the benchmark. In the intuitive rate scheme, the channel is considered as AWGN channel and the data rate,  $R_b$ , can be de-

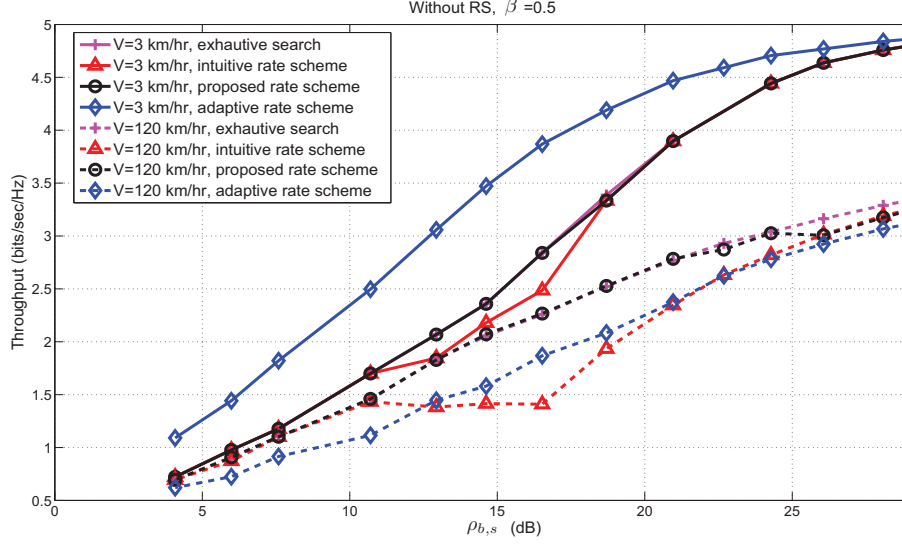


Figure 7.3: Compare the rate adaption schemes in different fading speed.

rived from,  $R_b = \log_2(1 + \rho)$ , where  $\rho$  denotes the average received SNR from RS at SS. From the simulation results, the proposed rate adaptation strategy is more close to the results of exhaustive search than intuitive rate scheme, and thus, it is more appropriate than intuitive rate scheme. In adaptive rate scheme, the BS will adjust the  $R_b$  adaptively according to the responding CSI. In other words,  $R_b = \frac{1}{T_p} \sum_{n=0}^{T_p} \log_2 \left\{ 1 + \frac{a^{2(n-1)} \rho |\mathbf{H}|^2}{1 + [1 - a^2] \rho} \right\}$  where  $|\mathbf{H}|^2$  denotes the responding CSI from SS. Due to the adaptive mechanism, the throughput of adaptive rate scheme is the best in the  $V=3$  km/hr case. However, the benefit of adaptive mechanism only exists in the slow fading channels. When  $V=120$  km/hr, the throughput becomes the worst because the responding CSI is outdated. These results show that the adaptive mechanism is sensitive to the fading effect. In contrast to the adaptive rate scheme, the proposed rate scheme is more robust to the fading effect. For example, the adaptive

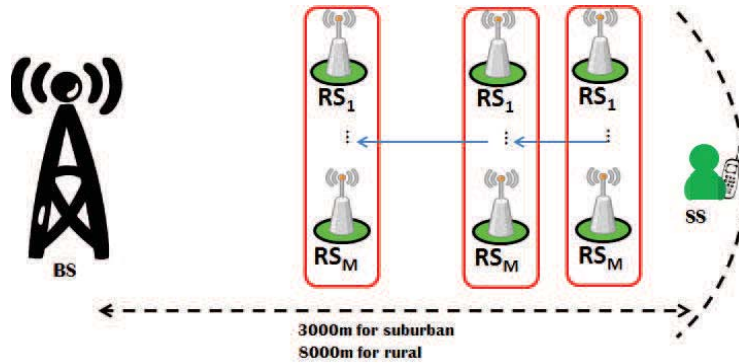


Figure 7.4: Topology for the case with multiple RSs. The coverage is 3 km and 8km for suburban and rural area, respectively

rate scheme needs extra 10 dB SNR gain to oppose the fading effect if the requirement of throughput is 2.5 bits/sec/Hz. However, 3 dB SNR gain is enough to oppose the fading effect for proposed rate scheme. Based on the feature of robust, the proposed rate scheme is used in the investigation.

### 7.1.2 Relay-Assisted Network

The topology of relay-assisted network is illustrated in Fig. 7.4. The cell coverage in suburban and rural environment is 3000 m and 8000 m, respectively. The SS is located on the cell boundary and the  $M$  RSs are located between the BS and the SS. Based on the topology, Fig. 7.5 shows the maximum available throughput can be twice of the case without RS even only the single RS is used to implement the ARQ relaying scheme. From the results, the packet retransmission through RS is conducive to enhance the throughput. However, the benefit of ARQ relaying scheme only exists when the RS is close to the SS enough. The fading speed still affect the

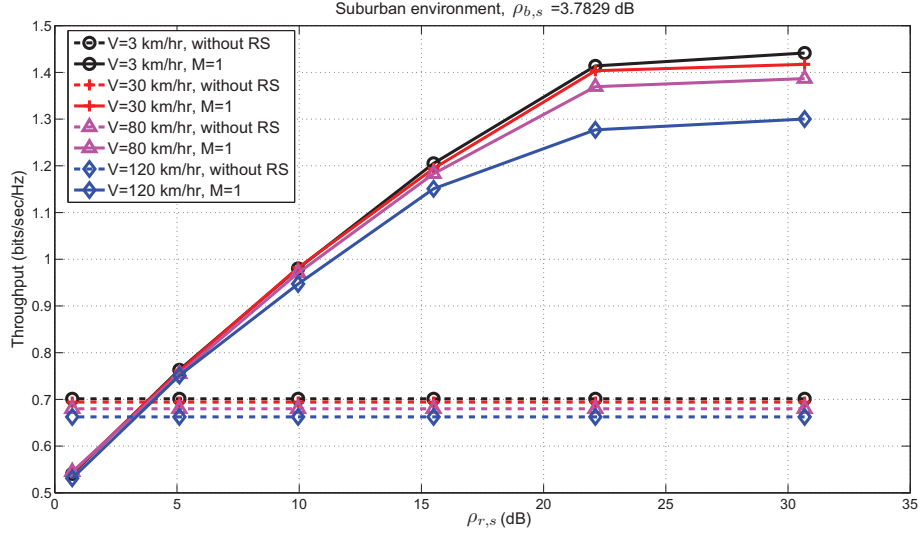


Figure 7.5: The throughput enhancement by single RS.

throughput in relay assisted network. In addition, the efficiency of ARQ relaying scheme is relative to the fading speed. From the simulation results, the RS can provide more help for enhancing the network throughput in slow fading channels.

The throughput with respect to the number of RS, fading speed and opportunistic gain is presented in Fig 7.6. As shown in the figure, the throughput will increase with the number of RS regardless of the fading speed, because the packet arrival rate, (6.14), at RS will increase while the number of RS grows from one to four. In other words, more packets can be resent by RS as long as the queue of RS is stable. In addition, the retransmission through the RS is more conducive to enhance the throughput than the BS. Thus, increasing the number of RS can improve the throughput.

In addition to raising the number of RS, opportunistic gain also can

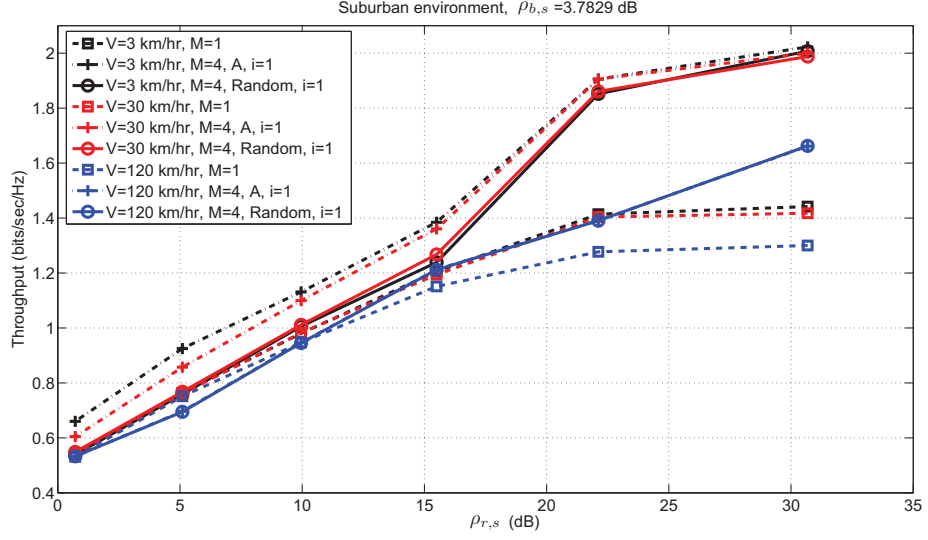


Figure 7.6: The throughput performance with different number of RSs, fading speed.

enhance the throughput. Except for the  $V=120$  km/hr case, the throughput for Type-A protocol is higher than the random selection scheme which the RS is selected randomly by BS. However, the benefit of opportunistic relaying on throughput is reduced with increasing the fading speed. If the delay on feedback is longer than the channel coherence interval, the responding CSI is outdated for selecting RS. Therefore, the opportunistic gain does not exist in fast fading channels. The throughput of Type-A scheme and random selection scheme is not distinguishable when  $V=120$  km/hr.

By inheriting the results of Fig. 7.6, the simulation results of the three proposed opportunistic relaying protocols, Type-A, Type-B and Type-C, are presented in Fig. 7.7 when  $i = 1$  in the suburban environment. As introduced in Chapter 4, Type-B protocol can obtain the opportunistic gain in each time

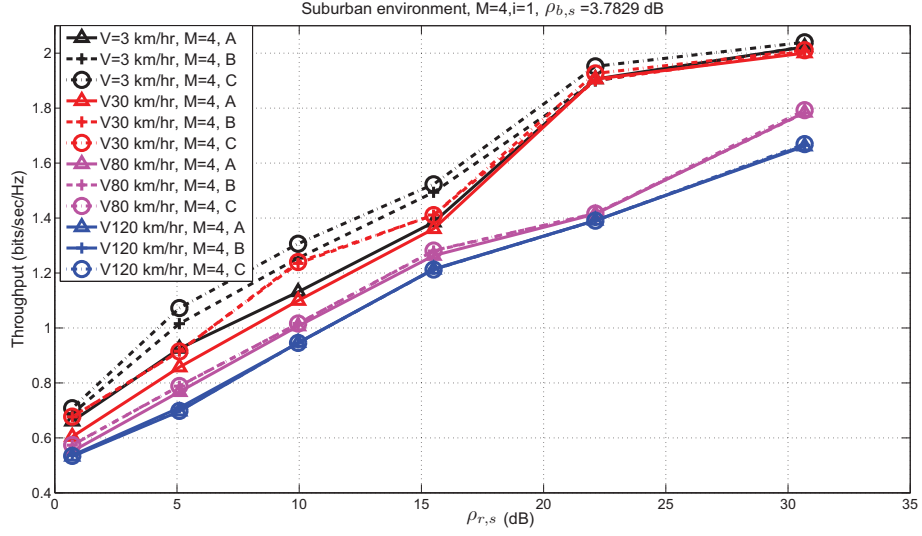


Figure 7.7: The throughput performance for different types of protocol in different fading speed.

of retransmission but Type-A only obtains the opportunistic gain in the first retransmission. On the other hand, Type-B is the same as Type-A while losing the opportunistic gain. Thus, there is an obvious gap between Type-A and Type-B in slow fading channel especially when  $V=3$  km/hr. In the case of  $V=80$  and  $V=120$ , the throughput of Type-A and Type-B are almost the same. Similarly, Type-C can be approached to Type-B for  $i = 1$  case if the opportunistic gain does not exist. Thus, the throughput of Type-B and Type-C is the same in fast fading channels.

Except for the number of RS, the throughput is relative to the  $i$  for using ODSTC $i$  scheme and the simulation results are presented in Fig. 7.8 and Fig. 7.9 for the case  $V=120$  km/hr and  $V=3$  km/hr, respectively. Due to the loss of the opportunistic gain, Type -A,B and C are almost the same



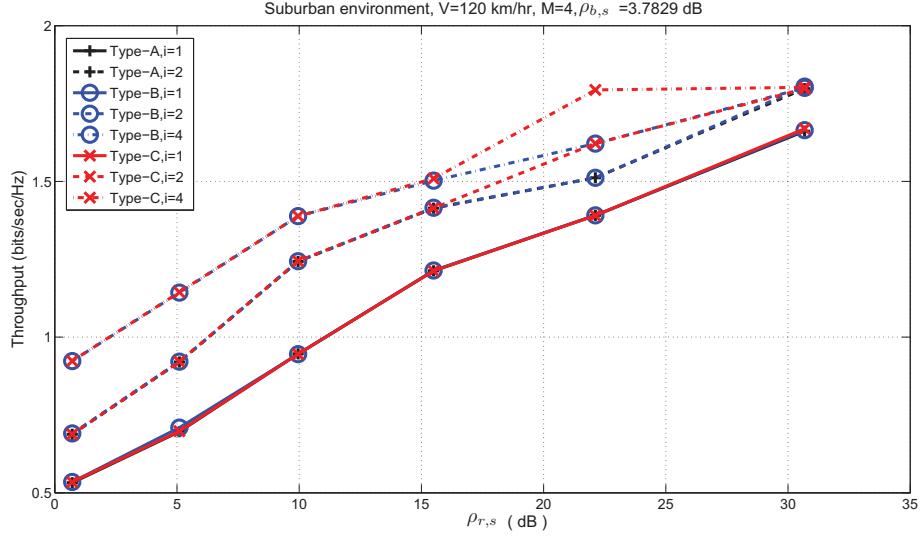


Figure 7.8: The throughput with different types of protocol in different  $i$  when  $V=120$  km/hr.

in  $V=120$  km/hr. In addition, the loss of the opportunistic gain will cause that the ODSTC scheme is degenerated to the DSTC scheme in  $V=120$  km/hr. Thus, the throughput will be enhanced significantly by increasing  $i$  for ODSTC $i$  scheme in Fig. 7.8. Similarly, the throughput of Type-C is possibly higher than those of Type-A and Type-B when  $i > 2$ . Especially when  $i = M$  in Type-A and Type-B, the opportunistic gain is limited when  $\mathcal{D} < i$ . However,  $\mathcal{S}_{\mathcal{D}}$  will keep growing in Type-C because the RSs are allowed to overhear from each other. Thus, the higher opportunistic gain can be achieved in Type-C than other ARQ relaying protocols. As shown in 7.8, the Type-C protocol with  $i = 4$  has a obvious throughput gain at  $SNR_{r,s} \approx 23$  dB. However, Type-B and Type-C is similar in almost case. Thus, opportunistic relaying is not a good choice from the viewpoint of the

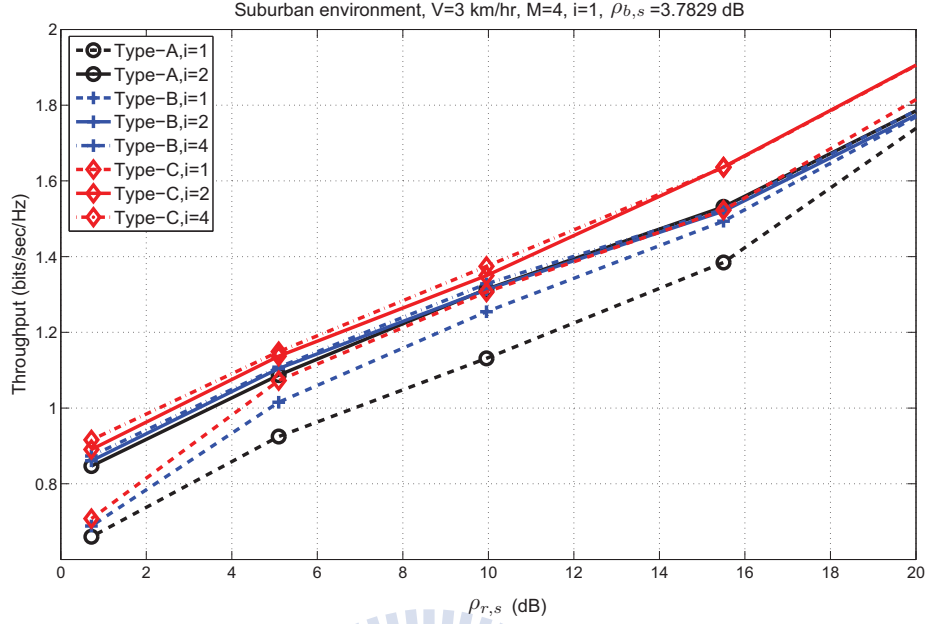


Figure 7.9: The throughput with different types of protocol in different  $i$  when  $V=3$  km/hr.

protocol complexity in fast fading channels.

In  $V=3$  km/hr case, the opportunistic gain can be obtained while using the ODSTC $i$  scheme. Fig. 7.9 shows that the difference between  $i = 4$  and  $i = 2$  is almost indistinguishable. Thus,  $i = 2$  is a better choice than  $i = 4$  in  $V=3$  km/hr from the perspective of the transmitting efficiency. Due to the opportunistic gain, the advantage of RS reselection is obvious and shown in the gap between Type-B and Type-A protocol. In contrast to fast fading channels, the gain of overhearing in Type-C is magnified especially when the RS is far away from BS due to the benefit of RS reselection.

According to the simulation so far, Fig. 7.10 shows the summarization of the appropriate relaying protocol for different fading speed. In fast fading

RS location Fading speed	Close to BS	Far away from BS
<b>Fast fading channels</b> ( $V=120,80$ km/hr)	Random selection, $i=4$	Random selection, $i=4$
<b>Slow fading channels</b> ( $V=3,30$ km/hr)	Type-B, $i=2$	Type-C, $i=2$

Figure 7.10: The recommended opportunistic relaying scheme.

speed, the opportunistic relaying scheme is able to be abandoned, but large size of the DSTC scheme is necessary. In slow fading, the benefit of opportunistic relaying is obvious. In order to enhance the system throughput, opportunistic relaying protocol is needed. From the perspective of transmitting efficiency, Type-B  $i = 2$  or Type-C  $i = 2$  will be needed in the slow fading case according to the distance between the BS and the RS. Fig. 7.11 shows the comparison of throughput between the perspectives of cross-layer design and PHY layer. From the results, there is a obvious gap between numerical analysis and the simulation regardless of the fading speed. In the numerical result, the CSI is always available when using the ODSTC scheme due to free negotiating delay, neglecting uncertainty, and the opportunistic gain always exists without considering the queue stability of RS. However, the negotiating delay, channel uncertainty in the fading speed and queue stability of RS are considered from the perspective of cross-layer design. Thus, the throughput of numerical results in  $V=120$  km/hr case will greater than the simulation results. In addition to queue stability of RS and opportunis-

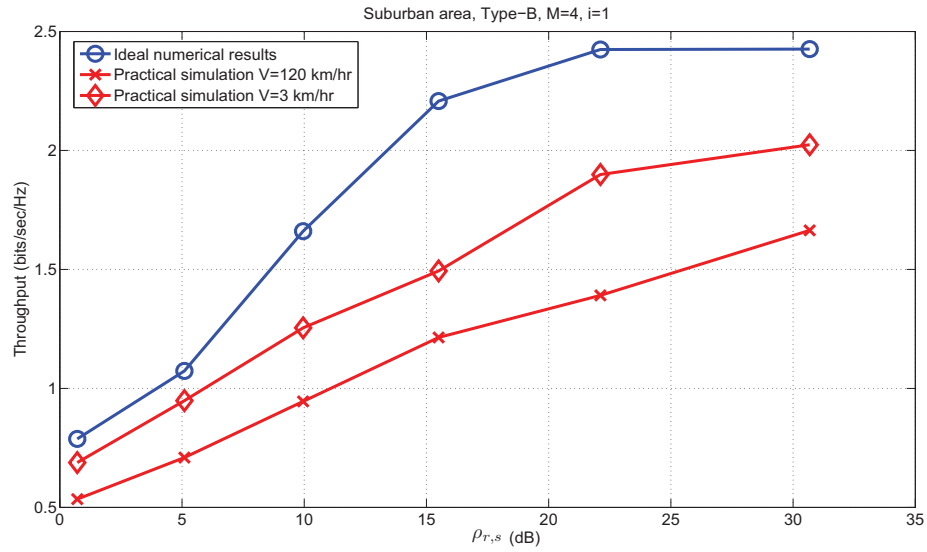


Figure 7.11: The difference between ideal numerical result and simulation results.

tic gain, under the assumption that the block fading channel independently frame by frame, the temporal diversity always exists in every retransmission regardless of fading speed. Thus, the numerical results are still better in  $V=3$  km/hr because the temporal diversity does not exist frame by frame from the perspective of cross-layer design. The discussion about Fig. 7.11 can be summarized in the in the Fig. 7.12.

Fading speed	Slow fading channels ( $V=3,30$ km/hr)	Fast fading channels ( $V=80,120$ km/hr)
Ideal numerical results	★●◆▼	★●◆▼
Practical simulation results	◆	▼

- ★ denotes the benefits without considering the channel uncertainty
- denotes the benefits without considering the queue stability
- ◆ denotes the benefits of opportunistic gain
- ▼ denotes the benefits of frame by frame temporal diversity

Figure 7.12: The comparisons between ideal numerical result and practical simulation result .

# Chapter 8

## Conclusions

By inheriting the idea of opportunistic relaying from [8], three types of MAC protocol which includes cooperative relaying and ODSTC schemes are proposed in the work. The behavior of these ARQ relaying protocols, such as fixed relaying in Type-A, RS re-selection in Type-B and overhearing in Type-C, are different and correspond to different performance of retransmission and complexity. Moreover, the critical difference between [8] and this work is that the negotiating delay, fading effect, uncertainty and queue stability of RS were considered from the perspective of cross-layer design. Based on the three MAC protocol, the tradeoff between throughput and complexity were re-evaluated from the perspective of the cross-layer design in this work.

According to the simulation results, the fading effect influences the performance of opportunistic relaying scheme significantly. Thus, there is no different between the throughput between of Type-A, Type-B, Type-C and random selection in the case of  $V = 120$  km/hr due to the loss of opportunistic gain. In order to improve the performance of ARQ relaying, increasing

$i$  for ODSTC $i$  scheme and the number of RS,  $M$ , can raise the throughput significantly. The contribution of opportunistic gain to throughput is more and more significant with the fading speed decreases. In the case of  $V=3$  km/hr case, there is a obvious gap on throughput between opportunistic relaying and random selection. The benefit of opportunistic relaying causes the throughput of Type-B greater than that of Type-A, and the gap between different size of the ODSTC is reduced. In addition to the opportunistic diversity, the temporal diversity also influences the throughput. Due to the loss of temporal diversity, the throughput in  $V=3$  km/hr is possibly less than  $V=120$  km/hr when opportunistic relaying is not used.

Overall, the opportunistic gain can provide significant contribution to enhancing the throughput. However, the performance of opportunistic relaying will be influenced by fading effect. From the view point of the transmitting efficiency, the scheme which abandons the opportunistic relaying scheme and raised the size of DSTC is appropriate for increasing throughput in fast fading channels. In slow fading channels, the large  $i$  for using ODSTC $i$  is not an efficient scheme for throughput enhancement. From the simulation results, Type-B protocol with  $i = 2$  is a better scheme for slow fading channels when the RS is close to the BS. If the RS is far away from BS, Type-C protocol with  $i = 2$  case is better than Type-B due to growing cardinality of the decoding set.

# Chapter 9

## Appendices

### 9.1 Appendix 1

Based on (6.19), the outage probability  $\tilde{P}(R, \rho, 1/2)$  is defined as  $\tilde{P}(R, \rho, 1/2) \triangleq \Pr \left\{ R < \tilde{C}(T_p, \rho, 1/2) \right\}$ . According to the definitions, we derive the outage probability of BS-RSs link, BS-SS link and RSs-SS link in the following.

#### 9.1.1 The Outage Probability of BS-RSs link and BS-SS link

$$\begin{aligned} \tilde{P}_{bs}(R_b, \rho_{b,s}, 1/2) &= \Pr \left\{ \tilde{C}(T_p, \rho, 1/2) < R_b \right\} \\ &= \Pr \left\{ \frac{1}{2} \left[ \log_2(1 + |h_{b,s}|^2 \rho_{b,s}) + \log_2(1 + |h_{b,s}|^2 \sigma_{T_p}) \right] < R_b \right\} \end{aligned}$$



where  $\frac{a^{2(T_p-1)}SNR_{b,s}}{1+(1-a^{2(T_p-1)})\rho_{b,s}} = \sigma_{T_p}$

$$\begin{aligned}
\Rightarrow \tilde{P}_{bs}(R_b, \rho_{b,s}, 1/2) &= \Pr \left\{ \log_2 \left[ (1 + |h_{b,s}|^2 \rho_{b,s}) \times (1 + \sigma_{T_p} |h_{b,s}|^2) \right] < 2R_b \right\} \\
&= \Pr \left\{ (\sigma_{T_p} \rho_{b,s})^2 |h_{b,s}|^4 + (\sigma_{T_p} + \rho_{b,s}) |h_{b,s}|^2 - (2^{2R_b} - 1) < 0 \right\} \\
&= \Pr \left\{ \frac{-(\rho_{b,s} + \sigma_{T_p}) - \sqrt{(\rho_{b,s} + \sigma_{T_p})^2 + 4(2^{2R_b} - 1)\rho_{b,s}\sigma_{T_p}}}{2\rho_{b,s}\sigma_{T_p}} < \right. \\
&\quad \left. |h_{b,s}|^2 < \frac{-(\rho_{b,s} + \sigma_{T_p}) + \sqrt{(\rho_{b,s} + \sigma_{T_p})^2 + 4(2^{2R_b} - 1)\rho_{b,s}\sigma_{T_p}}}{2\rho_{b,s}\sigma_{T_p}} \right\}
\end{aligned}$$

1.  $\rho_{b,s} > 0$

2.  $1 \geq a^2 > 0$ , if the fading speed is slower than 1608.401 km/hr

$$\Rightarrow \sigma_{T_p} = \frac{a^{2(T_p-1)}\rho_{b,s}}{1+(1-a^{2(T_p-1)})SNR_{b,s}} > 0$$

3.  $R_b > 0 \Rightarrow 2^{2R_b} - 1 > 0$

From 1,2,3

$$\begin{aligned}
\Rightarrow \frac{-(\rho_{b,s} + \sigma_{T_p}) - \sqrt{(\rho_{b,s} + \sigma_{T_p})^2 + 4 \times (2^{2R_b} - 1)\rho_{b,s} \times \sigma_{T_p}}}{2\rho_{b,s}\sigma_{T_p}} < 0 \\
\Rightarrow \frac{-(\rho_{b,s} + \sigma_{T_p}) + \sqrt{(\rho_{b,s} + \sigma_{T_p})^2 + 4 \times (2^{2R_b} - 1)\rho_{b,s} \times \sigma_{T_p}}}{2\rho_{b,s}\sigma_{T_p}} > 0
\end{aligned}$$

Therefore,

$$\begin{aligned}
\tilde{P}_{bs}(R_b, \rho_{b,s}, 1/2) &= \Pr \{ 0 \leq |h_{b,s}|^2 < \eta_{b,s} \} \\
&= 1 - e^{-\eta_{b,s}}
\end{aligned} \tag{9.1}$$

where  $\eta_{b,s} = \frac{-(\rho_{b,s} + \sigma_{T_p}) + \sqrt{(\rho_{b,s} + \sigma_{T_p})^2 + 4(2^{2R_b} - 1)\rho_{b,s}\sigma_{T_p}}}{2\rho_{b,s}\sigma_{T_p}}$

Similarly, we can derive the outage probability of BS and  $m$ -th RS link, which is denoted as  $\tilde{P}_{b,r}(R_b, \rho_{b,r}, 1/2)$  by

$$\begin{aligned}\tilde{P}_{b,r}(R_b, \rho_{b,r}, 1/2) &= \Pr \{0 \leq |h_{b,r_m}|^2 < \eta_{b,r_m}\} \\ &= 1 - e^{-\eta_{b,r_m}}\end{aligned}\quad (9.2)$$

where  $\eta_{b,r_m} = \frac{-(\rho_{b,r_m} + \sigma_{T_p}) + \sqrt{(\rho_{b,r_m} + \sigma_{T_p})^2 + 4(2^{2R_b} - 1)\rho_{b,r_m} \cdot \sigma_{T_p}}}{2\rho_{b,r_m} \sigma_{T_p}}$

### 9.1.2 The Outage Probability of RSs-SS link

The BS transmits one packet to SS unsuccessfully. There are  $D$  RSs correctly overhear the packet. Therefore, the  $D$  RSs have ability to retransmit the packet by data rate  $R_r$ . According to the channel quality, the BS wants to select the best  $i$  RSs among the  $D$  RSs to retransmit the packet. Under the situation, we want to derive the outage probability  $\widetilde{P}_{O_i|D}(R, \rho_{r,s}, 1/2|d)$  by ODSTC*i*.

$$\widetilde{P}_{O_i|D}(R, \rho_{r,s}, 1/2|d) = \Pr \left\{ \widetilde{C}(T_p, \rho, i, 1/2) < R_r \right\} \quad (9.3)$$

Where

$$\begin{aligned}\widetilde{C}(T_p, \rho, i, 1/2) &= \frac{1}{2} \log \left( 1 + \sum_{j=\max\{1, d-i+1\}}^d |X_j|^2 \rho_{r,s} \right) \\ &+ \frac{1}{2} \log \left( 1 + \frac{a^{2(T_r-1)} \sum_{j=\max\{1, d-i+1\}}^d |X_j|^2 \rho_{r,s}}{1 + (1 - a^{2(T_r-1)}) \rho_{r,s}} \right)\end{aligned}\quad (9.4)$$

I. When  $1 \leq i \leq d$

$$\begin{aligned} & \widetilde{C}_{T_r}(i) \\ = & \frac{1}{2} \left\{ \log\left(1 + \sum_{j=d-i+1}^d |X_j|^2 \rho_{r,s}\right) + \log\left(1 + \frac{a^{2(T_r-1)} \sum_{j=d-i+1}^d |X_j|^2 \rho_{r,s}}{1 + (1 - a^{2(T_r-1)}) \rho_{r,s}}\right) \right\} \end{aligned}$$

$$\text{lets } \sigma_{T_r} = \frac{a^{2(T_r-1)} \rho_{r,s}}{1 + (1 - a^{2(T_r-1)}) \rho_{r,s}}$$

$$\begin{aligned} \widetilde{P}_{\mathcal{O}_i|D}(R, \rho_{r,s}, 1/2|d) &= Pr \left\{ \widetilde{C}(T_p, \rho, i, 1/2) < R_r \right\} \\ &= Pr \left\{ \frac{1}{2} [\log(1 + |X_S|^2 \rho_{r,s}) + \log(1 + \sigma_{T_r} |X_S|^2)] < R_r \right\} \\ &\Rightarrow Pr \left\{ \frac{-(\rho_{r,s} + \sigma_{T_r}) - \sqrt{(\rho_{r,s} + \sigma_{T_r})^2 + 4(2^{2R_r} - 1)\rho_{r,s}\sigma_{T_r}}}{2\rho_{r,s}\sigma_{T_r}} < \right. \\ &\quad \left. |X_S|^2 < \frac{-(\rho_{r,s} + \sigma_{T_r}) + \sqrt{(\rho_{r,s} + \sigma_{T_r})^2 + 4(2^{2R_r} - 1)\rho_{r,s}\sigma_{T_r}}}{2\rho_{r,s}\sigma_{T_r}} \right\} \end{aligned}$$

Due to

1.  $\rho_{r,s} > 0$
2.  $1 \geq a^2 > 0$ , if the fading speed is slower than 1608.401 km/hr  $\Rightarrow \sigma_{T_r} = \frac{a^{2(T_r-1)} \rho_{r,s}}{1 + (1 - a^{2(T_r-1)}) \rho_{r,s}} > 0$

3.  $R_r > 0 \Rightarrow 2^{2R_r} - 1 > 0$

From 1, 2, 3

$$\begin{aligned} &\Rightarrow \frac{-(\rho_{r,s} + \sigma_{T_r}) - \sqrt{(\rho_{r,s} + \sigma_{T_r})^2 + 4 \times (2^{2R_r} - 1)\rho_{r,s}\sigma_{T_r}}}{2\rho_{r,s}\sigma_{T_r}} < 0 \\ &\Rightarrow \frac{-(\rho_{r,s} + \sigma_{T_r}) + \sqrt{(\rho_{r,s} + \sigma_{T_r})^2 + 4 \times (2^{2R_r} - 1)\rho_{r,s}\sigma_{T_r}}}{2\rho_{r,s}\sigma_{T_r}} \geq 0 \end{aligned}$$

Therefore,

$$\begin{aligned}
\widetilde{P}_{\mathcal{O}_i|D}(R, \rho_{r,s}, 1/2|d) &= \Pr \{0 \leq |X_{\mathbf{S}}|^2 \\
&< \frac{-(\rho_{r,s} + \sigma_{T_r}) + \sqrt{(\rho_{r,s} + \sigma_{T_r})^2 + 4(2^{2R_r} - 1)\rho_{r,s}\sigma_{T_r}}}{2\rho_{r,s}\sigma_{T_r}} \} \\
&= \Pr \{0 \leq |X_{\mathbf{S}}|^2 < \eta_{r,s}\} \tag{9.5}
\end{aligned}$$

where  $\eta_{r,s} = \frac{-(\rho_{r,s} + \sigma_{T_r}) + \sqrt{(\rho_{r,s} + \sigma_{T_r})^2 + 4(2^{2R_r} - 1)\rho_{r,s}\sigma_{T_r}}}{2\rho_{r,s}\sigma_{T_r}}$ . Replace  $|X_{\mathbf{S}}|^2$  by  $\sum_{j=d-i+1}^d |X_j|^2$ ,

$$\Rightarrow \widetilde{P}_{\mathcal{O}_i|D}(R, \rho_{r,s}, 1/2|d) = \Pr \left\{ 0 \leq \sum_{j=d-i+1}^d |X_j|^2 < \eta_{r,s} \right\} \tag{9.6}$$

The CCDF of the term  $\sum_{j=d-i+1}^d |X_j|^2$  is derived at (5.5). Applying (5.5) to (9.6)

$$\begin{aligned}
\widetilde{P}_{\mathcal{O}_i|D}(R, \rho_{r,s}, 1/2|d) &= \Pr \left\{ 0 \leq \sum_{j=d-i+1}^d |X_j|^2 < \eta_{r,s} \right\} \\
&= 1 - \Pr \left\{ \sum_{j=d-i+1}^d |X_j|^2 \geq \eta_{r,s} \right\} \\
&= 1 - \sum_{j=1}^{d-i} a_j e^{\left(\frac{-c_j}{i} \eta_{r,s}\right)} \times \frac{1}{(-b_j)^i} \left[ 1 - e^{b_j \eta_{r,s}} \sum_{\ell=0}^{i-1} \frac{(-b_j \eta_{r,s})^\ell}{\ell!} \right] \\
&\quad + \sum_{k=0}^{i-1} e^{(-\eta_{r,s})} \frac{(\eta_{r,s})^k}{k!} \tag{9.7}
\end{aligned}$$

**II.** When  $i > D$

$$\begin{aligned}
\widetilde{P_{\mathcal{O}_i|D}}(R, \rho_{r,s}, 1/2|d) &= \Pr \left\{ 0 \leq \sum_{j=1}^d |X_j|^2 < \eta_{r,s} \right\} \\
&= 1 - \sum_{k=0}^{i-1} e^{(-\eta_{r,s})} \frac{(\eta_{r,s})^k}{k!}
\end{aligned} \tag{9.8}$$



# Bibliography

- [1] P. Liu, Z. Tao, S. Narayanan, T. Korakis, and S. Panwar, “CoopMAC: A Cooperative MAC for Wireless LANs,” *IEEE Journal on Selected Areas in Communication*, vol. 25, no. 2, 2007.
- [2] H. Zhu and G. Cao, “rDCF: A Relay-Enabled Medium Access Control Protocol for Wireless Ad Hoc Networks,” *IEEE Trans. on Mobile Computing*, vol. 5, no. 9, pp. 1201–1214, 2006.
- [3] *IEEE standard for local and metropolitan area networks part 16: Task Group m (TGm)*, Apr. 2009, available at <http://www.ieee802.org/16/tgm>.
- [4] *Third-Generation partnership project’s (3GPP) long term evolution (LTE): Release 10 & beyond (LTE-Advanced)*, May 2009, available at <http://www.3gpp.org/LTE-Advanced>.
- [5] J. N. Laneman and G. W. Wornell, “Distributed space-time coded protocols for exploiting cooperative diversity in wireless networks,” *IEEE Trans. on Information Theory*, vol. 49, no. 10, pp. 2415–2525, 2003.

- [6] A. Bletsas, H. Shin, and M. Win, “Cooperative communications with outage-optimal opportunistic relaying,” *IEEE Trans. on Wireless Communications*, vol. 6, no. 9, pp. 3450–3460, 2007.
- [7] P. Zhang, F. Wang, Z. Xu, S. Diouba, and L. Tu, “Opportunistic distributed space-time coding with semi-distributed relay selection method,” *Research Journal of Information Technology*, vol. I, pp. 41–50, 2009.
- [8] H.-L. Chiu, S.-H. Wu, and J.-H. Li, “Cooperative ARQs with opportunistic distributed space-time coding: Effective protocols and performance analysis,” in *Proc. IEEE Information Theory Workshop (ITW)*. Dublin, Ireland, Aug 2010.
- [9] N. Li, N. Cheng, X. Xu, and Y. Cai, “Performance analysis of the cooperative communications based on opportunistic relaying from MAC layer perspectives,” in *Proc. IEEE International Conference on Communication Technology (ICCT)*. Nanjing, China, Nov 2010.
- [10] *IEEE standard for local and metropolitan area networks part 16: Air interface for fixed and mobile broadband wireless access systems: Multihop relay specification*, P802.16j/D9, May 2009, available at <http://www.ieee802.org/16>.
- [11] C. Nie, P. Liu, T. Korakis, E. Erkip, and S. Panwar, “CoopMAX: A Cooperative MAC with Randomized Distributed Space-Time Coding for an IEEE 802.16 Network,” in *Proc. IEEE ICC*. Dresden, Germany, Jun 2009.

- [12] L.-K. Chiu and S.-H. Wu, “The achievable rate of the training-based MIMO systems over time-varying fading channels: a BCRB perspective on channel tracking,” in *Proc. IEEE ICC*. Kyoto, Japan, June 2011.
- [13] Q. Zhang and S. A. Kassam, “Finite-State Markov Model for Rayleigh Fading channel,” *IEEE Trans. on Communications*, vol. 47, no. 11, pp. 1688–1692, 1999.
- [14] Mobile Broadband Wireless Communication Laboratory, *Technical report*, Institute of Communications Engineering, National Chiao Tung University, Hsinchu, Taiwan.
- [15] IEEE 802.16 Broadband Wireless Access Group, *IEEE 802.16m-08/003r7, The Draft IEEE 802.16m System Description Document*, Feb. 2009, available at <http://www.ieee802.org/16>.
- [16] IEEE 802.16 Broadband Wireless Access Group, *Multihop relay system evaluation methodology (channel model and performance metric)*, Feb. 2007, available at <http://www.ieee802.org/16>.